Solar Physics

# Kuramoto model of non-linear coupled oscillators as a way to understand phase synchronization: application to solar and geomagnetic indices.

--Manuscript Draft--

| | |
|---|---|
| **Manuscript Number:** | |
| **Full Title:** | Kuramoto model of non-linear coupled oscillators as a way to understand phase synchronization: application to solar and geomagnetic indices. |
| **Article Type:** | Original Research |
| **Keywords:** | "nonlinear oscillators", "solar activity", "geomagnetic indices", "coupling", "phase synchronization" |
| **Corresponding Author:** | Elena Blanter, Ph.D.<br>Institute de Physique du Globe<br>Paris, FRANCE |
| **Corresponding Author Secondary Information:** | |
| **Corresponding Author's Institution:** | Institute de Physique du Globe |
| **Corresponding Author's Secondary Institution:** | |
| **First Author:** | Elena Blanter, Ph.D. |
| **First Author Secondary Information:** | |
| **Order of Authors:** | Elena Blanter, Ph.D. |
| | Jean-Louis Le Mouël, Prof. |
| | Mikhail Shnirman, Ph.D. |
| | Vincent Courtillot, Prof. |
| **Order of Authors Secondary Information:** | |
| **Abstract:** | We apply a Kuramoto model of nonlinear coupled oscillators to the simulation of slow variation of the phase difference between sunspot number R_I and geomagnetic indices aa and \zeta . Kuramoto model is described in the particular case of two oscillators connected by a symmetric coupling with a quasi-stationary behavior. We deduce a relationship between the coupling and correlation properties of a pair of indices. We investigate the influence of the high-frequency variations in the amplitude of indices to the Kuramoto Model Reconstruction (KMR). Solving an inverse problem we reconstruct the evolution of coupling between pairs of indices (R_I and aa, R_I and \zeta , aa and \zeta ), and interpret it in terms of solar dynamo. The de-correlation between R_I and geomagnetic indices found in 20th solar cycle by Le Mouël et al (2012) is successfully reproduced by the Kuramoto model and corresponds to a change of leading oscillator. Application of the Kuramoto model to the cross-correlations C(R_I,\zeta) and C(aa,\zeta) for \zeta indices computed in 8 geomagnetic stations shows latitudinal dependence of the mean phase difference. We discuss obtained results in terms of the solar wind contribution to local geomagnetic indices \zeta . |

Powered by Editorial Manager® and ProduXion Manager® from Aries Systems Corporation

*Manuscript
Click here to download Manuscript: kuramoto_sp1.docx

# Kuramoto model of non-linear coupled oscillators as a way to understand phase synchronization: application to solar and geomagnetic indices.

Elena M. Blanter[1,2], Jean-Louis Le Mouël[1], Mikhail G. Shnirman[1,2], Vincent Courtillot[1]

[1]*Institut de Physique du Globe, Paris, France*

[2]*Institute of Earthquake Prediction Theory and Mathematical Geophysics, RAS, Moscow, Russia*

blanter@ipgp.fr

We apply a Kuramoto model of nonlinear coupled oscillators to the simulation of slow variation of the phase difference between sunspot number $R_I$ and geomagnetic indices aa and $\zeta$. Kuramoto model is described in the particular case of two oscillators connected by a symmetric coupling with a quasi-stationary behavior. We deduce a relationship between the coupling and correlation properties of a pair of indices. We investigate the influence of the high-frequency variations in the amplitude of indices to the Kuramoto Model Reconstruction (KMR). Solving an inverse problem we reconstruct the evolution of coupling between pairs of indices ( $R_I$ and aa, $R_I$ and $\zeta$, aa and $\zeta$ ), and interpret it in terms of solar dynamo. The de-correlation between $R_I$ and geomagnetic indices found in 20th solar cycle by Le Mouël et al (2012) is successfully reproduced by the Kuramoto model and corresponds to a change of leading oscillator. Application of the Kuramoto model to the cross-correlations $C(R_I, \zeta)$ and $C(aa, \zeta)$ for $\zeta$ indices computed in 8 geomagnetic stations shows latitudinal dependence of the mean phase difference. We discuss obtained results in terms of the solar wind contribution to local geomagnetic indices $\zeta$.

*Key words: nonlinear oscillators, solar activity, geomagnetic indices, coupling, phase synchronization*

## Introduction

Solar activity is reflected in different proxies and indices: number and areas of sunspots and of their groups; coronal activity; radio and UV/EUV radio emission; characteristics of Interplanetory Magnetic Field (IMF) and solar wind; cosmic rays; geomagnetic indices etc. These indices are quite different at short time scales (hours, days, months), but show an evident similarity at decadal time scale due to the Schwabe solar cycle. However, the correlation between them at annual and decadal time scale is not constant, and periods of high synchronization may be succeeded by periods of de-correlation. This non-stationary

synchronization of indices may lead, for example, to a high variability in the forecasting of the next solar cycle maximum when predictions are based on different solar proxies and methods (see e.g. Pesnel, 2008; Petrovay, 2010). The origin of synchronized and de-synchronized periods in the solar dynamics is to be found in nonlinear features of solar dynamo. However the concrete mechanism is far from being understood, and the relative contribution of low and high-frequency solar variability in the coherence of the different indices is unknown. In the present paper we focus on their slow phase evolution as a possible origin of the de-correlation periods of usually well correlated indices.

In our previous work (Le Mouël et al, 2012) we have found an extreme de-correlation event between geomagnetic and sunspot indices in the 20$^{th}$ solar cycle. The present work has the ambition to find a mechanism explaining these observed de-synchronizations. The most well-known common phenomenon inducing a similarity between solar and geomagnetic indices is the 11-year solar cycle. Relying on this common periodicity, we propose to consider synchronization and de-synchronization between indices in terms of phase coherence.

An approach based on the phase coherence was suggested as a new measure of the North-South asymmetry of sunspot activity (Zolotova and Ponyavin, 2006). In s following work of Donner and Thiel (2007), the phase coherence between North and South hemispheres was analyzed through the evolution of two nonlinear coupled oscillators. It was found that the North-South phase coherence is observed only for oscillations with periods between 7 and 14 years, i.e. in the period range of the solar cycle. In general, the phase difference between sunspot activity in North and South hemispheres is not a constant feature, and periods when the North hemisphere is leading alternate with periods when the South hemisphere takes the lead (Zolotova et al, 2010).

In the present work we use the concept of nonlinear coupled oscillators with the view of the variations of sunspot number and geomagnetic indices are representative of those of the toroidal and poloidal components of solar magnetic field. As in Donner and Thiel (2007) analysis, we do not require the existence of two real oscillators because they may be successfully replaced by two relevant indices. The evolution of the phase difference between sunspot number and *aa*

indices was investigated by Paluš and Novotná (2009) using Fourier analysis, and a quasi periodical behavior of the phase difference with a period of about 36 years was found. In the present paper, we aim to find a model of nonlinear coupled oscillators that could reproduce the synchronizations and de-synchronizations of indices observed in Le Mouël et al (2012) by means of a slow evolution of the phase difference.

One of the simple models describing the synchronization phenomenon in a system of nonlinear coupled oscillators is the Kuramoto model (Acebron et al, 2005). In this model the phase evolution of a system of oscillators is determined by a system of nonlinear differential equations. We describe a particular case of the Kuramoto model restricted to two nonlinear coupled oscillators with symmetric coupling. The phase evolution is determined by the evolution of the coupling between the oscillators. Coming to the solar magnetic field, we assume that the coupling between the toroidal and poloidal components of the solar magnetic field determines the evolution of the phase difference between sunspot number and aa indices. Before applying the Kuramoto model to solar and geomagnetic indices we have no a priori information on the possible coupling between the toroidal and poloidal components of the magnetic field, and, consequently, about the possible connection between solar and geomagnetic indices. However we do have information on the evolution of the cross-correlation between indices (Le Mouel et al, 2012). Thus we solve the inverse problem consisting in computing the coupling in a Kuramoto model that produces an evolution of the cross-correlation between simulated series similar to the evolution of the cross-correlation observed for actual indices.

The paper is organized as follows: in Section 2 we briefly present solar and geomagnetic data series and the evolution of the cross-correlation between them. Section 3 is devoted to the relationship between the phase difference and the cross-correlation between sine series depending on additive or multiplicative noise affecting its amplitude. Section 4 describes the considered Kuramoto model and its direct solutions. In Section 5 we construct the inverse problem solution for cases of sine series with a constant phase difference. In Section 6 we indicate how the quality of the Kuramoto reconstruction is measured and consider the case of series simulated by a Kuramoto type model with periodically evolving coupling.

Section 7 contains the application of the Kuramoto model to the inverse problem solution for solar and geomagnetic series described in Section 2. Discussion and interpretation of results are presented in Section 8. Extended mathematical calculations are moved to the Appendix.

## 2. Indices and their synchronization

In this paper we consider the same indices as in Le Mouel et al (2012), namely sunspot number series ( $R_I$ ), *aa*-index and $\zeta$ index – a local geomagnetic index similar to *Dst* index that can be easily computed at any geomagnetic observatory. All data are daily sampled. In order to reduce high-frequency oscillations and influence of annual, semi-annual and daily variations, we consider centered annual running means of daily indices. Resulting series are also daily sampled but their high-frequency component is significantly reduced. The evolution of the cross correlation between those smoothed indices is computed within 11-years centered running window.

### 2.1. Data

The *aa* index is a range index estimating the maximal magnetic disturbance within 3 hour intervals. The *aa*-index was introduced by Mayaud (Mayaud, 1972), its construction is based on data from two roughly antipodal observatories: Greenwich (and its successors Abinger and Hartland) and Melbourne (and its successor Toolangi). We use here the daily *aa* values, which are the averages of the 8 three-hourly *aa* values for the day. The daily aa series for the time span 1868 – 2011 is available through The International Service of Geomagnetic Indices (ISGI), gateway http://isgi.latmos.ipsl.fr/source/indices/aa/ .

In order to have local indices similar to *Dst* index, we built and use $\zeta$-indices (Le Mouël et al, 2004). The $\zeta$-index is a local index relevant to a given geomagnetic observatory. It is determined as the absolute value of the 3-day slope of the horizontal component H of geomagnetic field. The $\zeta$- indices correlate well with *Dst*, but cover a longer time span (Le Mouël et al, 2012, Shnirman et al, 2010). In the present study we consider 8 observatories that provide long and homogeneous geomagnetic series without long gaps: Alibag (1925 – 2011), Eskdalemuir (1911 – 2010), Honolulu (1902 – 2010), Kakioka (1924 – 2010),

Lerwick (1926 – 2010), Sitka (1902 – 2010), San Juan (1926 – 2010) and Tucson (1909 – 2010). These data are available through the World Data Centre for Geomagnetism (WDC) in Edinburgh http://www.wdc.bgs.ac.uk/catalog/master.html.

As long direct solar indices, we use the International Sunspot number series ($R_I$) recorded daily without any gap (1850 – 2011) ftp://ftp.ngdc.noaa.gov/STP/SOLAR_DATA/SUNSPOT_NUMBERS/INTERNATIONAL.

### 2.2. Synchronization and de-synchronization between indices at decennial time scale

All considered indices show the 11-year solar cycle, which appears in geomagnetic series as a result of the forcing by the solar magnetic field. The solar cycle governs the quasi-periodicity of solar and geomagnetic indices and accounts for their similarity at decennial time scale. However, the solar magnetic field contributes different geomagnetic indices in different ways, and the indices are not always synchronized: e.g., it is well-known that $R_I$ and *aa* indices reach their maxima at different phases of a solar cycle. The time lag between their maxima is about 2-3 years and varies from cycle to cycle. This phase difference of sunspot number and *aa* indices is an important phenomenon reflecting features of the behavior of the solar dynamo field ingredients (toroidal and poloidal), and it is widely used in solar cycle prediction. We monitor the phase difference variation of these indices through the change of their mutual correlation (Le Mouël et al, 2012). The most prominent de-synchronization event happens during the anomalous 20$^{th}$ solar cycle: sunspot number $R_I$ and *aa* indices, presenting usually a high positive correlation become anti-correlated during this cycle (Figure 1). At the same time other geomagnetic indices (*Dst* and $\zeta$) de-correlate with both $R_I$ and *aa*-indices (see figures in Le Mouël et al, 2012).

Various factors of the de-correlation between indices observed in the 20$^{th}$ solar cycle may be evoked: variation of the phase difference between indices, variation of the cycle length, increased high-frequency noise in its amplitude or frequency, abrupt change of regime. In the present paper we investigate the first factor. Variations of the cycle length are closely connected with our problem

because it is very difficult to separate variations in phase and variations in period. We do not study thoroughly the de-correlation which could be due to changes in the high-frequency components (noise) of amplitude or frequency affecting the solar cycle. Indeed, the Kuramoto model which we use for the simulation of slow variations of the phase difference between indices does not reproduce the high-frequency variations; however, the quality of the reconstructions of slow variations of the phase difference is affected by the amplitude of the high-frequency noise (Section 4).

## 3. Phase difference and correlation of sine series

Let us start with some simple examples of periodic series affected by a stochastic noise – additive and multiplicative. Let $X_0(t)$ and $Y_0(t)$ be two sine series with the same period $T = \frac{2\pi}{\Omega}$ and a constant phase difference $\Psi_0 = \Psi_1 - \Psi_2$:

$$\begin{cases} X_0(t) = a_X \sin(\Omega t + \Psi_1) + b_X \\ Y_0(t) = a_Y \sin(\Omega t + \Psi_2) + b_Y \end{cases} \quad (1)$$

The sliding cross-correlation between $X_0(t)$ and $Y_0(t)$ computed over an interval of length $T$ centered on $t$ is:

$$C_0(t) = C_T(X_0, Y_0) = \frac{\left\langle \left(X_0(\tau) - \langle X_0 \rangle_T\right)\left(Y_0(\tau) - \langle X_0 \rangle_T\right)\right\rangle_T}{\sqrt{\left\langle \left(X_0(\tau) - \langle X_0 \rangle_T\right)^2 \right\rangle \left\langle \left(Y_0(\tau) - \langle Y_0 \rangle_T\right)^2 \right\rangle}} = \\ = \frac{\int_{t-T/2}^{t+T/2} \left(X_0(\tau) - \langle b_X \rangle_T\right) d\tau \int_{t-T/2}^{t+T/2} \left(Y_0(\tau) - \langle b_Y \rangle_T\right) d\tau}{\sqrt{\int_{t-T/2}^{t+T/2} \left(X_0(\tau) - \langle b_X \rangle_T\right)^2 \left(Y_0(\tau) - \langle b_Y \rangle_T\right)^2 d\tau}} \quad (2)$$

When the coefficients $a$ and $b$ in Eq. (1) are constant, the sliding correlation between the two series $C_0(t) = C_T(X_0, Y_0)$ computed over an interval of length $T$ is expressed through the phase shift $\Psi_0$ as follows:

$$C_0(t) = \cos \Psi_0 \quad (3)$$

However, when some of the coefficients $a_X$, $a_Y$, $b_X$ and $b_Y$ are independent random values, then the sliding correlation is multiplied by a correction factor which depends on the characteristics of the distribution of those random values (see Appendix A for details).

### 3.1. Additive noise correction

Applying our estimations to real data we assume that the sampling rate (1) of series $X_0(t)$ and $Y_0(t)$ is small with respect to the length of the period of the oscillation $T$ ($T >> 1$). Let us assume coefficients $a_X$ and $a_Y$ to be constant and coefficients $b_X$ and $b_Y$ at each time moment $t$ to be independent random values with the same probability distribution and standard deviations $\sigma_X$ and $\sigma_Y$. As long as $T >> 1$ we can apply the central limit theorem and obtain the following expression for the sliding correlation between $X_0(t)$ and $Y_0(t)$ (Appendix A):

$$C_0(t) = \frac{\cos\Psi_0}{\sqrt{1+2\left(\frac{\sigma_X^2}{a_X^2}+\frac{\sigma_Y^2}{a_Y^2}\right)+4\frac{\sigma_X^2\sigma_Y^2}{a_X^2 a_Y^2}}} \quad (4)$$

### 3.2. Multiplicative noise correction

Let us now assume coefficients $b_X$ and $b_Y$ to be constant and coefficients $a_X$ and $a_Y$ to be independent random values with the same probability distribution with mathematical expectations $A_X$ and $A_Y$ respectively and relevant standard deviations $\sigma_X$ and $\sigma_Y$. The sliding correlation between $X$ and $Y$ will be then expressed as follows (Appendix A):

$$C_0(t) = \frac{\cos\Psi_0}{\sqrt{1+\left(\frac{\sigma_X^2}{A_X^2}+\frac{\sigma_Y^2}{A_Y^2}\right)+\frac{\sigma_X^2\sigma_Y^2}{A_X^2 A_Y^2}}} \quad (5)$$

We conclude that the sliding correlation of two series oscillating with the same period, estimated over an interval equal to this period, is proportional to $\cos\Psi_0$. Variations of correlation $C_0(t)$ may be related with variations of the phase difference between the series, $\Psi_0$, or with variations of parameters of the

probability distribution of the amplitude coefficients (e.g. $\sigma_X$ and $\sigma_Y$). The random part of the coefficients in Eq. (1) reduce the absolute value of the correlation.

## 4. Kuramoto model

Kuramoto model is generally used to study the synchronization between several nonlinear oscillators, more specifically, it describes the phase evolutions of a system of nonlinear coupled oscillators (see Strogatz, 2000 for review). We use here a particular simplified case of Kuramoto model adapted to the modeling of the evolution of the phase difference between two data series.

Let us consider two coupled oscillators with constant frequencies $\omega_1 = \Omega + \Delta\omega$ and $\omega_2 = \Omega - \Delta\omega$; the evolution of their phases $\theta_1 = \theta_1(t)$ and $\theta_2 = \theta_2(t)$ is supposed to be governed by the system of non-linear differential equations:

$$\begin{cases} \dot{\theta}_1(t) = \omega_1 + \dfrac{\kappa}{2} Sin\left(\theta_2(t) - \theta_1(t)\right) \\ \dot{\theta}_2(t) = \omega_2 + \dfrac{\kappa}{2} Sin\left(\theta_1(t) - \theta_2(t)\right) \end{cases} \tag{6}$$

The strength of the symmetric coupling between the two oscillators is given by the coefficient $\kappa$. The sum and the difference of above equations give:

$$\begin{cases} \dot{\theta}_1 + \dot{\theta}_2 = 2\Omega \\ \dot{\theta}_1 - \dot{\theta}_2 = 2\Delta\omega - \kappa \sin\left(\theta_1 - \theta_2\right) \end{cases} \tag{7}$$

The first equation in Eq. (7) has a solution independent of coupling:

$$\theta_1 + \theta_2 = 2\Omega t + const \tag{8}$$

The second equation in (7) determines the synchronization or de-synchronization between the two oscillators and depends on coupling $\kappa$. The phase difference $\theta = \theta_1 - \theta_2$ satisfies the differential equation:

$$\dot{\theta} = 2\Delta\omega - \kappa \sin\theta \tag{9}$$

which may be easily solved by separation of variables. It has the critical point $|\kappa| = |2\Delta\omega|$. Depending on the strength of coupling $\kappa$, there are two situations:

1) In the case of a weak coupling $\kappa^2 < 4\Delta\omega^2$ the derivative $\dot{\theta}$ keeps a constant sign and its absolute value is larger than $|2\Delta\omega - \kappa| \neq 0$. No stationary solution exists, phases $\theta_1$ and $\theta_2$ diverge.

2) In the case of a strong coupling $\kappa^2 > 4\Delta\omega^2$ we have the stationary solution $\dot{\theta} = 0$ and two possible values for the phase difference $-\pi \le \theta \le \pi$:

$$\theta = \begin{bmatrix} \arcsin\left(\dfrac{2\Delta\omega}{\kappa}\right) \\ \pi - \arcsin\left(\dfrac{2\Delta\omega}{\kappa}\right) \end{bmatrix} \qquad (10)$$

One of the stationary solutions in Eq. (10) is stable and determines the phase synchronization of the oscillators; the other solution is unstable. The stability of the stationary solution $\dot{\theta}(t) = 0$ is determined by the sign of the derivative of the right side of Eq. (9). The derivative is equal to $-\kappa\cos\theta$ and must be negative in order to make the stationary solution stable. Combining condition $-\kappa\cos\theta < 0$ with Eq. (10), we obtain all stable stationary solutions of the Kuramoto model depending on signs of $\Delta\omega$ and $\kappa$:

(1) when $\Delta\omega$ and $\kappa$ are positive, the only stable solution in the interval $[-\pi, \pi]$ is $\theta = \arcsin\left(\dfrac{2\Delta\omega}{\kappa}\right)$;

(2) when $\Delta\omega$ and $\kappa$ are negative, the stable solution on the interval $[-\pi, \pi]$ is $\theta = \pi - \arcsin\left(\dfrac{2\Delta\omega}{\kappa}\right)$;

(3) when $\Delta\omega$ is positive and $\kappa$ is negative, the stable solution is $\theta = \arcsin\left(\dfrac{2\Delta\omega}{\kappa}\right)$;

(4) when $\Delta\omega$ is negative and $\kappa$ is positive, the stable solution is $\theta = -\pi - \arcsin\left(\frac{2\Delta\omega}{\kappa}\right)$.

# 5. Application of Kuramoto model to an inverse problem solution

When investigating the evolution of the correlation of e.g. two solar indices we generally lack information about the coupling connecting them. In order to get this information we solve an inverse problem and reconstruct this coupling through the Kuramoto model. Note that Eq. (6) governs the evolution of phases $\theta_1(t)$ and $\theta_2(t)$ of two oscillators having the same frequency $\Omega$, but provides no information about the evolution of their amplitudes.

Combining conditions on $\theta_1(t)$ and $\theta_2(t)$ given by Eqs (8) and (10), we define two synthetic series simulated by the Kuramoto model as:

$$\begin{cases} X(t) = \sin\left(\theta_1(t)\right) = \sin\left(\Omega t\right) \\ Y(t) = \sin\left(\theta_2(t)\right) = \sin\left(\Omega t + \theta(t)\right) \end{cases} \quad (11)$$

The sliding correlation $C(t)$ between the two series $X(t)$ and $Y(t)$ computed over a window of length $T = \frac{2\pi}{\Omega}$ is related to the phase difference $\theta = \theta_1 - \theta_2$ through Eq. (3), and can be compared with the correlation between real series $C_0(t)$.

Paragraphs 5.1 and 5.2 now describe how the coupling can be reconstructed from the evolution of the phase difference $\Psi_0(t)$ or the sliding correlation $C_0(t) = C_T\left(X_0, Y_0\right)$ when series $X_0(t)$ and $Y_0(t)$ are given by Eq. (1).

### 5.1. Reconstruction of coupling from the phase difference

Let us assume that we know the evolution of the phase difference $\theta_0(t)$ between the original series $X_0(t)$ and $Y_0(t)$. Without loss of generality, we take parameter $\Delta\omega$ positive and resolve Eq (9) as:

$$\kappa(t) = \frac{2\Delta\omega - \dot{\theta}_0(t)}{Sin(\theta_0(t))} \tag{12}$$

According to section 4.1 the stationary solution of Kuramoto model exists only in the case of strong coupling $\kappa^2 > 4\Delta\omega^2$. When the phase difference $\theta_0$ is constant and $\dot{\theta}_0(t) = 0$, this condition is guaranteed by Eq. (12), and the KMR is always successful. When $\dot{\theta}_0(t) > 0$ the coupling given by Eq. (12) may happen to be weak $\kappa^2(t) < 4\Delta\omega^2$, leading to the failure of the reconstruction. Thus, in the quasi-stationary case of a slowly evolving phase difference $\theta_0(t)$, the reconstruction of the coupling $\kappa(t)$ is successful in a neighborhood of the stationary solution $\dot{\theta}_0(t) = 0$.

### 5.2. Reconstruction of coupling from sliding correlation

When the phase difference between the two series $X_0(t)$ and $Y_0(t)$ is not known, we replace it with the sliding correlation $C_0(t) = C_T(X_0, Y_0)$. Indeed, in the case when the evolution of $X_0(t)$ and $Y_0(t)$ is given by Eq. (1) with constant coefficients, the phase difference $\theta_0(t)$ is directly obtained from the sliding correlation $C_0(t)$ by Eq. (3). However, when a high-frequency noise is present in the series $X_0(t)$ and $Y_0(t)$, it will enter the relationship between $\theta_0(t)$ and $C_0(t)$ (see Eqs. (4) and (5)).

In order to determine the coupling $\kappa(t)$ in the general case, let us introduce the *virtual* phase difference $\varphi_0(t)$ defined by the following condition:

$$C_0(t) = \cos(\varphi_0(t)) \tag{13}$$

When the series $X_0(t)$ and $Y_0(t)$ contain no noise and the phase difference $\theta_0$ between them is constant, the virtual phase $\varphi_0(t)$ is equal to $\theta_0$. When the phase difference $\theta_0(t)$ is not constant, the virtual phase $\varphi_0(t)$ represents a quasi-stationary estimate of $\theta_0(t)$.

There are two possible solutions of Eq. (13) depending of which oscillator in Eq. (6) (first or second) is leading:

$$\varphi_0(t) = \arccos\left(C_0(t)\right) \text{ or } \varphi_0(t) = -\arccos\left(C_0(t)\right) \tag{14}$$

Now we use Eq. (12) to get the coupling from the phase $\varphi_0(t)$. Replacing $\varphi_0(t)$ by its expression in function of $C_0(t)$ according to Eq. (14) we obtain the two solutions:

$$\kappa = \frac{2\Delta\omega - \left(\arccos\left(C_0(t)\right)\right)'}{Sin\left(\arccos\left(C_0(t)\right)\right)} \text{ or } \kappa = -\frac{2\Delta\omega + \left(\arccos\left(C_0(t)\right)\right)'}{Sin\left(\arccos\left(C_0(t)\right)\right)} \tag{15}$$

When correlation $C_0(t) = C_0$ is constant we always get a successful reconstruction. The two solutions (15) are anti-symmetrical and correspond to a change of the leading oscillator in Eq. (6) or to a change of sign of parameter $\Delta\omega$. The full expression for fixed $\Delta\omega$ will then be:

$$\left.\begin{aligned} \varphi_0 &= \arccos\left(C_0\right) \\ \kappa &= \frac{2\Delta\omega}{Sin\left(\arccos\left(C_0\right)\right)} \end{aligned}\right\} C_0 > 0$$

$$\left.\begin{aligned} \varphi_0 &= -\arccos\left(C_0\right) \\ \kappa &= -\frac{2\Delta\omega}{Sin\left(\arccos\left(C_0\right)\right)} \end{aligned}\right\} C_0 < 0 \tag{16}$$

The coupling is anti-symmetric with respect to positive and negative correlation $C_0$ and performs a jump from $-2\Delta\omega$ to $2\Delta\omega$ when correlation pass 0, increasing from -1 to 1 (Figure 2, red curve).

When the correlation $C_0(t)$ is not constant, Eq. (16) takes the form:

$$\left.\begin{aligned} \varphi_0(t) &= \arccos\left(C_0(t)\right) \\ \kappa(t) &= \frac{2\Delta\omega - \left(\arccos\left(C_0(t)\right)\right)'}{Sin\left(\arccos\left(C_0(t)\right)\right)} \end{aligned}\right\} C_0(t) > 0$$

$$\left.\begin{aligned} \varphi_0(t) &= -\arccos\left(C_0(t)\right) \\ \kappa(t) &= \frac{-2\Delta\omega - \left(\arccos\left(C_0(t)\right)\right)'}{Sin\left(\arccos\left(C_0(t)\right)\right)} \end{aligned}\right\} C_0(t) < 0 \tag{17}$$

The coupling in Eq. (17) is no longer anti-symmetric and its asymmetry depends on the sign of the derivative $\left(\arccos\left(C_0(t)\right)\right)'$ (Figure 2, blue and green curves). The necessary condition of strong coupling $\kappa^2 > 4\Delta\omega^2$ applied to Eq. (17) gives a restriction on the time variation of the correlation that should be fulfilled in order to have a successful reconstruction:

$$\left|\left(\arccos\left(C_0(t)\right)\right)'\right|^2 < 4\Delta\omega^2 \tag{18}$$

Eq (18) gives a condition on the acceptable range of $C_0'(t)$ inside which the Kuramoto model can be applied.

## 6. Quality of the Kuramoto model reconstruction (KMR)

Let us assume that we have solved the inverse problem with a Kuramoto model, i.e. have reconstructed the coupling $\kappa(t)$ from the sliding correlation $C_0(t) = C_T\left(X_0, Y_0\right)$ between two series $X_0(t)$ and $Y_0(t)$. Knowing the coupling $\kappa(t)$, we can simulate two series $X(t)$ and $Y(t)$ according to Eq. (11) with the phase difference $\theta(t)$ solution of Eq. (7). The sliding correlation $C(t) = C_T\left(X, Y\right)$ is the reconstruction of the correlation $C_0(t) = C_T\left(X_0, Y_0\right)$ by the Kuramoto model. We have now to estimate the quality of this reconstruction. Such an estimate requires that we introduce a measure quantifying the distance between the original correlation $C_0(t)$ and its reconstruction $C(t)$.

In this section we define two measures characterizing the quality of the Kuramoto model reconstruction (KMR) and present two illustrative examples. In the first example (Section 6.1), we solve the inverse problem for two series $X_0(t)$ and $Y_0(t)$ given by Eq. (1) and use the coupling reconstructed by Eq. (17) in order to generate two synthetic series $X(t)$ and $Y(t)$ by Eq. (11). In the second example we consider a Kuramoto model with a given coupling $\kappa_0(t)$ periodically evolving with period $L$, we model two phases $\Psi_1(t)$ and $\Psi_2(t)$ as solutions of

Eq. (6), simulate two series $X_0(t)$ and $Y_0(t)$ by Eq. (1) and reconstruct again the coupling $\kappa(t)$ from the correlation $C_0(t) = C_T(X_0, Y_0)$. These two examples are intended to show how the quality of the KMR depends on internal (period of the coupling's variations) and external (amplitude noise in original series $X_0(t)$ and $Y_0(t)$) parameters of the system of oscillators, before we apply it to real data series in Section 7.

### 6.1. Residual of the correlation

Let us consider two series $X_0(t)$ and $Y_0(t)$ given by Eq. (1) with an additive or multiplicative high-frequency noise on the amplitude (*a* or *b* are random values) and assume that the KMR of the coupling $\kappa(t)$ by Eq (17) is successful. Then we simulate two synthetic series $X(t)$ and $Y(t)$ with Eq. (11). As a natural measure quantifying the quality of the KMR we use the $L_2$-distance between sliding correlations $C_0(t) = C(X_0(t), Y_0(t))$ and $C(t) = C(X(t), Y(t))$. The residual $r(C)$ of the correlation is defined as follows:

$$r(C) = \frac{1}{W}\int \left(C_0(t) - C(t)\right)^2 dt \qquad (19)$$

The integral in Eq. (19) is taken over the whole time span *W* where series $X_0(t)$ and $Y_0(t)$ are defined. We take various values of the constant phase difference $\Psi_0$ between series $X_0(t)$ and $Y_0(t)$ and the same characteristics of the amplitude noise for $X_0(t)$ and $Y_0(t)$ in Eq. (1). The distance used by Eq. (19) linearly depends on $\cos(\Psi_0)$, as shown by Eqs. (4) and (5). In order to have a measure independent on $\Psi_0$ we introduce the relative residual equal to the relative $L_2$-distance between $C_0(t)$ and $C(t)$ normalizing Eq (19) to the squared standard deviation of $C_0(t)$:

$$r_0(C) = \frac{r(C)}{\sigma^2(C_0)} = \frac{\int \left(C_0(t) - C(t)\right)^2 dt}{\int \left(C_0(t) - \langle C_0(t)\rangle\right)^2 dt} \qquad (20)$$

Note that if we replace $C(t)$ in the nominator by the mean value of the original correlation $C_0(t)$ (i.e. $C(t)=\langle C_0(t)\rangle$), the relative residual will be equal to unity. This observation means that a successful reconstruction of the correlation requires values of the relative residual between zero and unity; otherwise, the quality of KMR is worse than that of a simple averaging.

Figure 3 shows characteristic values of residual and relative residual for two sine series given by Eq. (1) with the same constant amplitude $a_X = a_Y = A$ and two independent random values $b_X$ and $b_Y$ having the same dispersion $\sigma^2 = 1/12$. We present two examples with a constant phase difference, $\Psi_0 = 0.4$ and $\Psi_0 = 0.8$. In agreement with our theory, the residual $r(C)$ decreases with the growth of the sine amplitude $A$ and depends on the phase $\Psi_0$ (Figure 3a). The relative residual $r_0(C)$ also decreases when $A$ grows but it is independent on $\Psi_0$ (Figure 3b). Characteristic variations of the values of residual and relative residual are indicated by a standard deviation window; one hundred realizations are performed for Figure 3.

### 6.2 Residual of coupling

In this section we investigate how good we can reconstruct the coupling $\kappa(t)$ when two sine series $X_0(t)$ and $Y_0(t)$ are already generated by a Kuramoto model with a given coupling $\kappa_0(t)$. Applying the Kuramoto model to the correlation $C_0(t) = C(X_0, Y_0)$, we get the reconstructed coupling $\kappa(t)$, synthetic series $X(t)$ and $Y(t)$ (Eq. (11)), and their correlation $C(t) = C(X, Y)$. The quality of the Kuramoto reconstruction is characterized, as before, by the residual $r(C)$ and relative residual $r_0(C)$ defined by Eqs (19) and (20), but also by the distance between the original coupling $\kappa_0(t)$ and the reconstructed coupling $\kappa(t)$. Residual of coupling is defined as:

$$r(\kappa) = \frac{1}{W}\int \left(\kappa_0(t) - \kappa(t)\right)^2 dt \qquad (21)$$

and relative residual as:

$$r_0(\kappa)=\frac{\int\left(\kappa_0(t)-\kappa(t)\right)^2 dt}{\int\left(\kappa_0(t)-\left\langle\kappa_0(t)\right\rangle\right)^2 dt} \tag{22}$$

In order to see the influence of the form of coupling on the associate residual and relative residual, we consider a periodically evolving coupling $\kappa_0(t)$ relevant to the case of the phase difference oscillating with period $L$.

Let us consider a coupling of the form:

$$\kappa_0(t)=\frac{1-\frac{\pi D\Lambda}{2}\cos\Lambda t}{\sin\left(\pi\left(\frac{D}{2}\left(\sin\Lambda t+1\right)+c\right)\right)} \tag{23}$$

When $\Delta\omega=0.5$ the Kuramoto model with this coupling generates two series with a periodically evolving phase difference (see Eqs. (6) and (10)):

$$\Psi_0(t)=\Psi_1(t)-\Psi_2(t)=\pi\left(\frac{D}{2}\left(\sin\left(\Lambda t\right)+1\right)+c\right) \tag{24}$$

The phase difference is oscillating between its minimal and maximal value $\Psi_{\min}\le\Psi_0\le\Psi_{\max}$ where

$$\begin{cases}\Psi_{\min}=\pi c\\ \Psi_{\max}=\pi\left(D+c\right)\end{cases}$$

Let us choose parameters of coupling leading to a stable solution when $\Delta\omega$ and coupling $\kappa(t)$ are both positive. It means that the phase difference should be $0<\Psi_0<\pi$ (see Section 4, conditions of the stable stationary solution in case (1)), and therefore we have the following simple conditions on coefficients $D$ and $c$:

$$\begin{cases}0<c<1\\ 0<D<1-c\end{cases} \tag{25}$$

Simple computations show that under conditions (25) we always get a strong coupling when the period of the phase oscillation $L=\frac{2\pi}{\Lambda}$ is long enough.

Figure 4 shows how residual and relative residual of KMR of coupling and correlation decrease with the growth of period $L$. It presents Kuramoto modeling for coupling $\kappa_0(t)$ of Eq. (23) and series $X_0(t)$ and $Y_0(t)$ simulated by Eq. (1) with constant coefficients $a_X = a_Y = A$ and random coefficients $b_X$ and $b_Y$ with $\sigma^2 = 1/12$, and with phases being solutions of Eq. (6). Relative residuals become less than unity when the period $L$ of oscillations of the coupling $\kappa_0(t)$ becomes greater than 22 years ($L > 2T$). An example of the evolution of original coupling $\kappa_0(t)$ and reconstructed coupling $\kappa(t)$ when L=60 years is presented Figure 5a. Relevant correlation $C_0(t)$ and its reconstruction $C(t)$ are shown at Figure 5b. We see that $\kappa(t)$ follows well the shape and minima of $\kappa_0(t)$ but misses its highest values (Figure 5a). The overall reconstruction $\kappa(t)$ of coupling $\kappa_0(t)$ in Figure 5a is less good than the reconstruction $C(t)$ of the sliding correlation $C_0(t)$ in Figure 5b, in agreement with absolute values of residuals and relative residuals presented in Figure 4.

# 7. Application to solar indices

In this section we apply the Kuramoto modeling to the 11-year sliding correlations between pairs of solar and geomagnetic indices: WN and *aa*; $\zeta$ indices and *aa*-index, $\zeta$ indices and WN. The procedure of the Kuramoto model application is presented in a schematic form in Figure 6 (numbers inside yellow arrows indicate used equations). When the Kuramoto reconstruction is successful, we expect $\theta(t)$ to be an estimate of the low-frequency variation of the phase difference between solar indices of a pair and the relative residual $r_0(C)$ to charcaterize the contribution of the high-frequency component of $X_0(t)$ and $Y_0(t)$ to their de-synchronization.

### 7.1. Sunspot number $R_I$ and *aa* indices.

We start our study with the two series $-R_I$ and *aa* – whose phase difference is claimed to be slowly evolving with a quasi-period of about 36 years

(Paluš and Novotná, 2009). The Kuramoto modeling performed with 11-yr correlation $C_0(WN, aa)$ is successful and its coupling is presented in Figure 7a. A stable solution of Eq. (6) exists and determines the evolution of the phase difference $\theta(t)$ presented in Figure 7b. The sliding correlation $C(X,Y)$ between two synthetic series $X(t)$ and $Y(t)$ simulated by Eq. (11) with the phase difference $\theta(t)$ is compared in Figure 7c with the original sliding correlation $C_0(WN, aa)$. Initial conditions of Eq. (6) do not affect the phase evolution on long term and may be neglected (Figure 7d).

The relative residual of the reconstruction is reasonably good, $r_0(C) = 0.12$, which is illustrated by the similarity between original and reconstructed correlations, $C_0(WN, aa)$ and $C(X,Y)$ (Figure 7c). As expected, the reconstructed correlation $C(X,Y)$ follows the slow evolution of $C_0(WN, aa)$ but does not represent its high-frequency variations (Figure 7c). The de-correlation of 20$^{th}$ solar cycle is reproduced by the model (Figure 7c), which means that the observed de-synchronisation of $R_I$ and *aa* indices may be explained by a slow evolution of the phase difference between them. The reconstructed coupling (Figure 7a) is positive and constant almost everywhere, except for a time interval pertaining to the 20$^{th}$ solar cycle where it becomes negative. That means that the fall of correlation between $R_I$ and *aa* in the 20$^{th}$ solar cycle cannot be considered as an ordinary variation as those observed outside this cycle, since it requires a reversal of the sign of coupling.

In order to test the stability of the KMR we perform the same reconstruction for different values of $\Delta\omega$ and $T$. Figure 8 (upper panels) shows that relative residual and mean value of the phase difference reach relevant constant values when $\Delta\omega > 0.1$. The relative residual shows a flat optimum around $T = 12.6$ years; the mean phase reaches its minimum around $T = 10.6$ years (Figure 8, bottom panels). The overall variation of the mean phase and relative residual when period $T$ varies between 8 and 14 years is quite small. The form and the mean value of the reconstructed phase difference does not practically depend on the choice of $T$ in the range of possible values of solar cycle length.

### 7.2. ζ-indices.

We consider ζ-indices recorded at 8 geomagnetic stations (see Section 2 for the list of observatories). The ζ-indices de-correlate with sunspot number $R_I$ and *aa*-index at the same time of the 20$^{th}$ solar cycle when the de-correlation event between $R_I$ and *aa* occurs (Le Mouël et al, 2012), although this de-correlation is less pronounced; it varies with geomagnetic station. We apply the Kuramoto model to the 11-years sliding correlation between different ζ-indices and WN or between ζ-indices and aa indices. We make use of the ζ-index property to be a local geomagnetic index, and will see if the latitude of the geomagnetic station is essential in the de-correlation of ζ indices from $R_I$ and *aa*.

Figure 9 shows the reconstructed correlations (red curve) compared to the original sliding correlations $C_0(\zeta, aa)$ between $\zeta$ and *aa* –index (blue curve). Figure 10 shows the same for the correlations between $\zeta$ and $R_I$ index. High-frequency oscillations in the correlation of local geomagnetic indices $\zeta$ with *aa,* and more markedly with $R_I$, are visibly stronger than in the correlation between $R_I$ and *aa* themselves considered above (Figure 7c). The coupling relevant to couples $(R_I, \zeta)$ (Figure 11, blue curve) is overall positive and demonstrates high oscillations depending on the considered station. The form of the evolution of coupling relevant to pairs $(aa, \zeta)$ is less dependent of the geomagnetic station (Figure 11, red curve). In the 20$^{th}$ solar cycle it shows a change of sign in low and mid-latitude stations; this change is accompanied by strong variations and disappears for high-latitude stations (LER, SIT). This result is in a good agreement with latitudinal dependence of geomagnetic activity with solar wind suggested by Finch et al (2008).

Lower values of the relative residual presented in Figure 12 confirm the first impression from Figures 9 and 10 of a higher stability of the KMR of the correlation of ζ-indices with aa-index than of those with $R_I$ index. Values of the relative residual $r_0(C(R_I, \zeta))$ are approximately two times greater than that of $r_0(C(aa, \zeta))$ (Figure 12a and c), and do not depend on latitude of geomagnetic stations. In contrast to the relative residual the mean phase demonstrates a clear

variation with the latitude of the geomagnetic observatory, separating mid-latitude stations (ABG, HON, KAK, SJG, TUC) from high-latitude ones (ESK, LER, SIT) (Figure 12 b and d). We recall that the relative residual is independent of the phase difference between the series, but is sensitive to the signal/noise ratio, and conclude that the high-frequency noise in ζ indices does not depend on the latitude (Figure 12a, c), while the phase difference does (Figure 12b and d). Latitude dependence of the mean phase difference presented at Figures 12b and d shows a mirror symmetry for *aa* and $R_I$ indices. It indicates that the influence of the toroidal components on the geomagnetic field becomes weaker going from mid-latitude to polar stations when the influence of the poloidal component becomes stronger.

# 8. Discussion and conclusions

The successful solution of the inverse problem for determining the coupling $\kappa(t)$ by the Kuramoto model allows one to interpret the de-correlation between pair of indices obtained in (Le Mouël et al, 2012) in terms of a long-term evolution of the phase difference between two nonlinear coupled oscillators. The form and intensity of the reconstructed coupling shows that the de-synchronization between the indices which occurred during the 20$^{th}$ solar cycle is an exceptional event in a whole century of available observations. This de-correlation event is generated by a slow evolution of the phase difference between indices, and is not the result of high-frequency noise or short living impulses. In the present paper, Kuramoto model has been applied to solar and geomagnetic indices. We lead the discussion of our results along two directions: the general significance of the model characteristics, and its application to concrete indices.

## 8.1. General interpretation of model characteristics

The Kuramoto model approach presented in this paper has at least three main characteristics (coupling, relative residual and optimal period) essential to the physical interpretation of obtained results.

***Coupling.*** The coupling is a measure of the strength of the connection between two indices. Its evolution governs the synchronization or de-synchronization reflected in the sliding correlation. There are at least two possible

interpretations of coupling. It can be the strength of the interactions between two oscillators as suggested by the Kuramoto model in its classical form; we can, for example, expect that such an interaction exists between the toroidal and poloidal components of the solar magnetic field and is imaged by the coupling between WN and *aa* series. In general, when two oscillators are physically coupled, they may affect each other differently ($\kappa$ may be different in the two differential equations of Eq. (6)). Nevertheless, a common situation is the one in which the same forcing acts on both of them. In this case, the coupling may be considered as a measure of this common forcing and enters Eq. (6) symmetrically. The Kuramoto model with symmetric coupling representing a common forcing can be applied to the evolution of the cross-correlation between indices recorded at two geomagnetic stations, climatic parameters from two local regions etc.

***Relative residual.*** The relative residual is a measure of the quality of the Kuramoto reconstruction which allows one to estimate the level of the high-frequency variations in the two series, which degrade the reconstruction of the coupling; when the relative residual is higher the accuracy of the phase and coupling reconstruction is lower. In order to obtain the actual evolution of phase and coupling, we have first to reduce the level of noise in the considered series. Nevertheless, when long period variations of coupling or correlation are strong they are fairly reproduced by the Kuramoto reconstruction even if the high-frequency noise leads to high values of relative residual (see e.g. variations of coupling of $\zeta$ series in Figure 11).

***Period***. It is well known that the solar cycle has no exact period. Variations of its period length complicate the estimation of its phase by usual techniques. Although we assume the existence of an exact period in our series, the reconstructed phase and coupling do not depend on the choice of the period length in a wide range from 8 to 14 years. This stability allows the application of the Kuramoto model to quasi-periodic systems. Relative residual and mean phase for the pair $R_I$ and *aa* reach their minima for T between 10 and 13 years (Figure 8c and d). Additional investigations could be performed in order to see how the optima of the different characteristics of the Kuramoto model can be properly used for the estimations of periods in multi and quasi periodical systems.

### 8.2. Application to the solar magnetic field

Sunspot and geomagnetic time series are considered as indices representative of the solar magnetic field (e.g. Ruzmaikin and Feynman, 2001). The solar field has two main components: toroidal and poloidal. Coronal mass ejections (CMEs), which typically produce geomagnetic disturbances called sudden commencement storms are closely related with the toroidal component of solar magnetic field. Geomagnetic disturbances produced by recurrent storms whose period is related with the 27day solar rotation are well correlated with the poloidal component. Both kinds of magnetic disturbances are reflected in geomagnetic indices (e.g. Mayaud, 1980; Richardson et al, 2000; Menvielle and Marchaudon, 2007; Richardson and Cane, 2012). The transient solar wind is also closely related with the toroidal magnetic field, and the quasi-stationary solar wind with the poloidal magnetic field. The solar wind contribution to the geomagnetic activity at the Earth's surface depends on terrestrial latitude (Finch et al, 2008), we take advantage of the local nature of $\zeta$ index to characterize the variations with latitude of the solar wind influence by studying the mean phase difference of the couples $(R_I, \zeta)$ and $(aa, \zeta)$ (Figure 12).

The coupling reconstructed through the Kuramoto model from the evolution of 11y sliding correlation between WN and *aa* indices may lead to two hipothesis (see Section 8.1): it may reveal the strength of the connection between the evolutions of the toroidal and poloidal fields, as proposed above, or it may be characteristic of the toroidal field alone which contributes both indices. In order to discriminate between these two hypothesis, we apply the Kuramoto model to another pair of indices: $R_I$ and "poloidal" part of the *aa* index, $aa_P$. We adopt a very simple definition of $aa_P$ which implies that the "toroidal" part of *aa* is linearly related to $R_I$ and may be removed from the *aa* index (Ruzmaikin and Feynman, 2001):

$$aa_P(t) = aa(t) - 0.07R_I(t) - 5.17 \qquad (26)$$

The 11y sliding correlations and reconstructed couplings of the two pairs of indices ($R_I$ and $aa_P$, $R_I$ and *aa*) are presented in Figure 13. We see that removing the part common with $R_I$ from the *aa* index produces only a small

reduction in the absolute value of the coupling (Figure 13a): the coupling from $R_I$ and $aa_P$ has absolute values similar to the coupling from $R_I$ and *aa*. We conclude that the coupling $\kappa(R_I, aa)$ reflects mainly the connection between the toroidal and poloidal components of the solar magnetic field and not the common forcing of $R_I$ and *aa* indices. The de-correlation between indices occurring in the 20th solar cycle is then interpreted as a change of the leading oscillator. This may be is a rare event in the behavior of the two components of the solar magnetic field, but the change of leading oscillator is frequently observed for North and South solar hemispheres (Zolotova et al, 2010).

Solar magnetic field performs an indirect forcing on the geomagnetic activity through different kinds of solar wind. Overall positive coupling presented in Figure 11 means that both components of the solar magnetic field (toroidal and poloidal) contribute to $\zeta$ index at the same level. Their contributions demonstrate low-frequency variations (Figure 11) and depend on the latitude of the geomagnetic observatory (Figure 12). The reversal of the sign of coupling $\kappa(R_I, aa)$ occurring in the 20th solar cycle (Figure 7a) influences $\zeta$ indices and lead to simultaneous de-correlations (Figures 9 and 10). Although couplings $\kappa(aa, \zeta)$ manifest some attempts to reverse during the 20th solar cycle (Figure 11, red curves) these events are less strong and convincing compared with that of $\kappa(R_I, aa)$.

The evolution of the coupling shows a clear difference between mid-latitude and higher latitude geomagnetic stations. Forcing of $\zeta$-index by the poloidal field is greater in high-latitude stations (Figure 12). A larger contribution of the poloidal field to high-latitude stations agrees with results of Finch et al. (2008) where it was shown that the effect of the bulk slow speed of the solar wind *v* is higher for high geomagnetic latitudes. Although the change of the leading component occurring during the 20th solar cycle is reflected as a minimum in all correlations of $\zeta$-indices with WN and aa indices, however this change takes a form of a reversal of the sign of coupling only on pairs composed of *aa* and mid-latitude $\zeta$-indices.

# Appendix. Phase difference and sliding correlation.

### Constant coefficients

Let us consider two sine series with constant coefficients:

$$X_0(t) = a_X \sin(\Omega t + \Psi_1) + b_X$$
$$Y_0(t) = a_Y \sin(\Omega t + \Psi_2) + b_Y \qquad \text{(A1)}$$

The mean values of series $X_0(t)$ and $Y_0(t)$ computed over any interval of length $T = \frac{2\pi}{\Omega}$ will be:

$$\langle X_0(t)\rangle_T = b_X ; \langle Y_0(t)\rangle_T = b_Y \qquad \text{(A2)}$$

The sliding correlation within a window of length *T* writes:

$$C_0(t) = C_T(X_0, Y_0) = \frac{\langle (X_0(\tau) - b_X)(Y_0(\tau) - b_Y)\rangle_T}{\sqrt{\langle X_0(\tau) - b_X\rangle_T^2 \langle Y_0(\tau) - b_Y\rangle_T^2}} =$$
$$= \frac{a_X a_Y \int \sin(\Omega\tau + \Psi_1)\sin(\Omega\tau + \Psi_2)\, d\tau}{\sqrt{a_X^2 a_Y^2 \int \sin^2(\Omega\tau + \Psi_1)\, d\tau \int \sin^2(\Omega\tau + \Psi_2)\, d\tau}} =$$
$$= \frac{\int \cos(\Psi_1 - \Psi_2)\, d\tau - \int \cos(2\Omega\tau + \Psi_1 + \Psi_2)\, d\tau}{\sqrt{\int (1 - \cos(2\Omega\tau + 2\Psi_1))\, d\tau \int (1 - \cos(2\Omega\tau + 2\Psi_2))\, d\tau}} = \cos(\Psi_1 - \Psi_2)$$

Integrations above is performed over interval of length *T*.

### Additive noise correction

Let us now suggest that $b_X$ and $b_Y$ in Eq. (A1) are independent random variables with expectations $\mathrm{E}[b_X] = B_X$, $\mathrm{E}[b_Y] = B_Y$ and standard deviation $\sigma_X$ and $\sigma_Y$ respectively. Then

$$\langle X_0(t)\rangle_T = B_X ; \langle Y_0(t)\rangle_T = B_Y$$

We compute the sliding correlation between $X_0$ and $Y_0$ within a window of length *T*. The integration of the independent random variables may be performed separately; and the length of *T* is big enough to allow the expectation and standard deviation be given by to the central limit theorem:

$$\int (b_X - B_X) d\tau = 0, \int (b_Y - B_Y) d\tau = 0$$
$$\int (b_X - B_X)^2 d\tau = \sigma_X^2, \int (b_Y - B_Y)^2 d\tau = \sigma_Y^2$$

The correlation is then expressed as follows:

$$C_0(t) = C_T(X_0, Y_0) = \frac{\left\langle \left(X_0(\tau) - B_X\right)\left(Y_0(\tau) - B_Y\right)\right\rangle_T}{\sqrt{\left\langle X_0(\tau) - B_X\right\rangle_T^2 \left\langle Y_0(\tau) - B_Y\right\rangle_T^2}} =$$

$$= \frac{\int \left(a_X \sin\left(\Omega\tau + \Psi_1\right) + b_X - B_X\right)\left(a_Y \sin\left(\Omega\tau + \Psi_2\right) + b_Y - B_Y\right) d\tau}{\sqrt{\int \left(a_X \sin\left(\Omega\tau + \Psi_1\right) + b_X - B_X\right)^2 d\tau \int \left(a_Y \sin\left(\Omega\tau + \Psi_2\right) + b_Y - B_Y\right)^2 d\tau}} =$$

$$= \frac{a_X a_Y \int \cos\left(\Psi_1 - \Psi_2\right) d\tau}{\sqrt{\left(a_X^2 \int \sin\left(\Omega t + \Psi_1\right)^2 d\tau + \int \left(b_X - B_X\right)^2 d\tau\right)\left(a_Y^2 \int \sin\left(\Omega t + \Psi_2\right)^2 d\tau + \int \left(b_Y - B_Y\right)^2 d\tau\right)}} =$$

$$= \frac{a_X a_Y \cos\left(\Psi_1 - \Psi_2\right)}{2\sqrt{\left(\frac{a_X^2}{2} + \sigma_X^2\right)\left(\frac{a_Y^2}{2} + \sigma_Y^2\right)}} = \frac{\cos\left(\Psi_1 - \Psi_2\right)}{\left(1 + 2\left(\frac{\sigma_X^2}{a_X^2} + \frac{\sigma_Y^2}{a_Y^2}\right) + \frac{4\sigma_X^2\sigma_Y^2}{a_X^2 a_Y^2}\right)}$$

Let us note that in the present case of additive noise the correlation does not depends on the expectation of the additive random variable but is determined by the signal-noise ratios $\sigma_X / a_X$ and $\sigma_Y / a_Y$.

**Multiplicative noise correction**

Let now coefficients $b_X$ and $b_Y$ in Eq. (A1) be constant and coefficients $a_X$ and $a_Y$ be independent random values with expectations $\mathrm{E}[a_X] = A_X$, $\mathrm{E}[a_Y] = A_Y$ and standard deviation $\sigma_X$ and $\sigma_Y$ respectively. The averages of series $X_0(t)$ and $Y_0(t)$ computed over an interval of length *T* will be again given by Eq. (A2). We suppose again that T is big enough to apply the central limit theorem, and therefore:

$$\int a_X d\tau = A_X, \int a_Y d\tau = A_Y$$
$$\int \left(a_X^2 - A_X^2\right) d\tau = \sigma_X^2, \int \left(a_Y^2 - A_Y^2\right) d\tau = \sigma_Y^2$$

Thus, the sliding correlation computed over an interval of length *T* will be:

$$C_0(t) = C_T(X_0, Y_0) = \frac{\left\langle \left(X_0(\tau) - b_X\right)\left(Y_0(\tau) - b_Y\right)\right\rangle_T}{\sqrt{\left\langle X_0(\tau) - b_X\right\rangle_T^2 \left\langle Y_0(\tau) - b_Y\right\rangle_T^2}} =$$

$$= \frac{\int \left(a_X \sin\left(\Omega\tau + \Psi_1\right)\right)\left(a_Y \sin\left(\Omega\tau + \Psi_2\right)\right) d\tau}{\sqrt{\int \left(a_X \sin\left(\Omega\tau + \Psi_1\right)\right)^2 d\tau \int \left(a_Y \sin\left(\Omega\tau + \Psi_2\right)\right)^2 d\tau}} =$$

$$= \frac{\int a_X d\tau \int a_Y d\tau \int \cos\left(\Psi_1 - \Psi_2\right) d\tau}{\sqrt{\left(\int a_X^2 d\tau \int \sin\left(\Omega t + \Psi_1\right)^2 d\tau\right)\left(\int a_Y^2 d\tau \int \sin\left(\Omega t + \Psi_2\right)^2 d\tau\right)}} =$$

$$= \frac{A_X A_Y \cos\left(\Psi_1 - \Psi_2\right)}{\sqrt{\left(A_X^2 + \sigma_X^2\right)\left(A_Y^2 + \sigma_Y^2\right)}} = \frac{\cos\left(\Psi_1 - \Psi_2\right)}{\left(1 + \left(\frac{\sigma_X^2}{A_X^2} + \frac{\sigma_Y^2}{A_Y^2}\right) + \frac{\sigma_X^2 \sigma_Y^2}{A_X^2 A_Y^2}\right)}$$

# References


Acebron, J. A., Bonilla, L. L., Vicente, C. J. P., Ritort, F. and Spigler, R.:2005, *Rev. Mod. Phys.*, 77,137.

Donner, R. and Thiel, M. :2007, *Astronom. Astrophys*., 475, L33.

Finch, I. D., Lockwood, M. L. and Rouillard A. P.:2008, *Geophys. Res. Lett.*, 35, L21105.

Le Mouël, J.-L., Blanter, E., Shnirman, M. and Courtillot, V. :2012, *J. Geophys. Res.*, 117, A09103.

Mayaud, P. N.: 1972, *J. Geophys. Res.*, 77, 6870.

Mayaud, P. N. :1980, Derivation, Meaning, and Use of Geomagnetic Indices, Geophys. Monogr. Ser., vol. 22, AGU, Washington, D. C.

Menvielle, M., and Marchaudon, A. :2007, Astrophys. and Space Sci. Libr., vol. 344, 277.

Paluš, M. and Novotná, D. :2009, *Journal of Atmospheric and Solar-Terrestrial Physics*, 71, 923.

Pesnell, W. D.: 2008, Sol. Phys., 252, 209–220.

Petrovay, K.: 2010, *Living Rev. Solar Phys*., 7, lrsp-2010-6.

Richardson, I. G., Cliver, E. W., and Cane, H. V.:2000, *J. Geophys. Res.*, 105, 18203–18213

Richardson I.G., and Cane, H.V.:2012, J. Space Weather Space Clim. 2, A01.

Ruzmaikin, A., and Feynman, J.:2001, *J. Geophys. Res.*, 106, 15783.

Shnirman, M., Le Mouël, J.-L. and Blanter, E.:2010, Sol. Phys., 266, 159.

Strogatz, S. H.:2000, *Physica D* 143, 1.

Zolotova N. V., and Ponyavin D. I.:2006, Astron. and Astrophys., 449, L1.

Zolotova N.V., Ponyavin, D.I. Arlt, R.and Tuominen, I.:2010, Astron. Nachr. 331, 765 .

# Figure legends

**Figure 1.** 11-year sliding correlation between 1 y averaged solar activity $R_I$ and geomagnetic indices: *aa* (blue) and |Dst| (red).

**Figure 2.** Coupling of Kuramoto model as a function of correlation for a constant correlation (red), slowly increasing correlation (blue) and slowly decreasing correlation (green). Frequency window is $2\Delta\omega = 0.05$.

**Figure 3.** Quality of the Kuramoto reconstruction. Variation of residual (a) and relative residual (b) vs amplitude of signal for phase shift $\Psi = 0.4$ (red) and $\Psi = 0.8$ (blue). Solid line is relevant to mean value over several realizations; dashed curves show one standard deviation window of variability of different realizations.

**Figure 4**. Relationship between the quality of the Kuramoto reconstruction and period *L* of the coupling oscillation. Period of sine series is equal to $T = \frac{2\pi}{\Omega} = 11$ years. Parameters of Kuramoto model are A=10, D=0.6, c=0.1, $\Delta\omega = 0.4$.

**Figure 5.** Kuramoto reconstruction of coupling (a) and sliding correlation (b). Initial coupling and correlation are presented in blue, their reconstructions – in red. Parameters of the Kuramoto model are: $T = 11$ years, $L = 60$ years, A=10, D=0.6, c=0.1, $\Delta\omega = 0.4$.

**Figure 6.** Scheme of application of the Kuramoto model to pair of indices. Numbers inside yellow arrows indicate numbers of equations in the main text.

**Figure 7.** Kuramoto simulation performed with the 11-year sliding correlation $C_0\left(R_I, aa\right)$ and $\Delta\omega = 0.4$. (a) – evolution of the reconstructed coupling; (b) – evolution of the phase difference $\theta(t)$ (red) and the 11-y sliding correlation $C_0\left(R_I, aa\right)$ (blue); (c) – evolution of the 11y sliding correlation $C_0\left(R_I, aa\right)$ (blue) and its KMR (red); (d) – influence of initial value of the phase difference $\theta(t_0)$ on the evolution of $\theta(t)$ in the Kuramoto model: $\theta(t_0)$=0.42 (magenta), $\theta(t_0)$=0.67 (red), $\theta(t_0)$=1.07 (green). All windows are centered.

**Figure 8.** Influence of parameters $\Delta\omega$ (a,b) and period $T = \frac{2\pi}{\Omega}$ (c,d) on relative residual $r_0(C)$ (a,c) and mean phase $\langle\theta\rangle$ (b,d) of KMR applied to $R_I$ and *aa* series.

**Figure 9.** The evolution of 11y sliding correlations between *aa* and ζ series $C_0\left(aa, \zeta\right)$ (blue) and its KMR (red) for 8 geomagnetic stations. The window of correlation is centered.

**Figure 10.** The evolution of 11y sliding correlations between $R_I$ and ζ series $C_0\left(R_I, \zeta\right)$ (blue) and its KMR (red) for 8 geomagnetic stations. The window of correlation is centered.

**Figure 11**. Evolution of coupling based on 11-years sliding correlation of $\zeta$ -indices with $R_I$ $C_0\left(R_I, \zeta\right)$ (blue) and of $\zeta$ -indices with aa-index $C_0\left(aa, \zeta\right)$ (red). Parameter of the Kuramoto model is $\Delta\omega = 0.4$, all windows are centered

**Figure 12.** Dependence on latitude of the quality of the KMR of 11-years sliding correlation of $\zeta$ indices with *aa* (top panels) and $R_I$ (bottom panels). Relative residual (left panels) and mean reconstructed phase (right panels) are presented.

**Figure 13.** Evolution of coupling (a) and sliding correlation (b) between sunspot number $R_I$ and aa index (blue); between $R_I$ and $aa_P$ (red). The $aa_P$ is defined by Eq. (26) in main text. The 11-y sliding window is centered.

Figure1

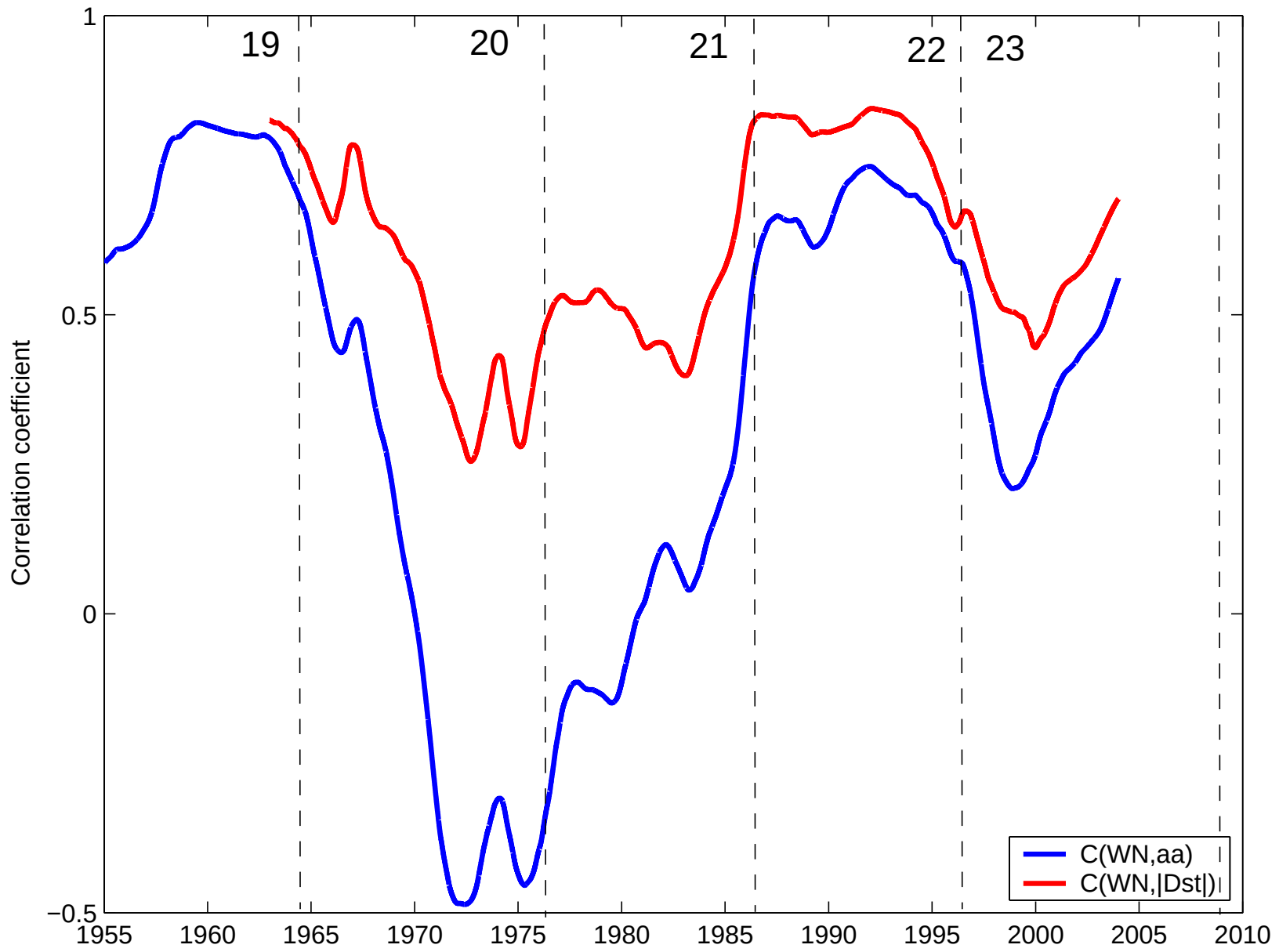
19
20
21
22
23
1
0.5
0
−0.5
Correlation coefficient
1955
1960
1965
1970
1975
1980
1985
1990
1995
2000
2005
2010
C(WN,aa)
C(WN,|Dst|)

Figure2

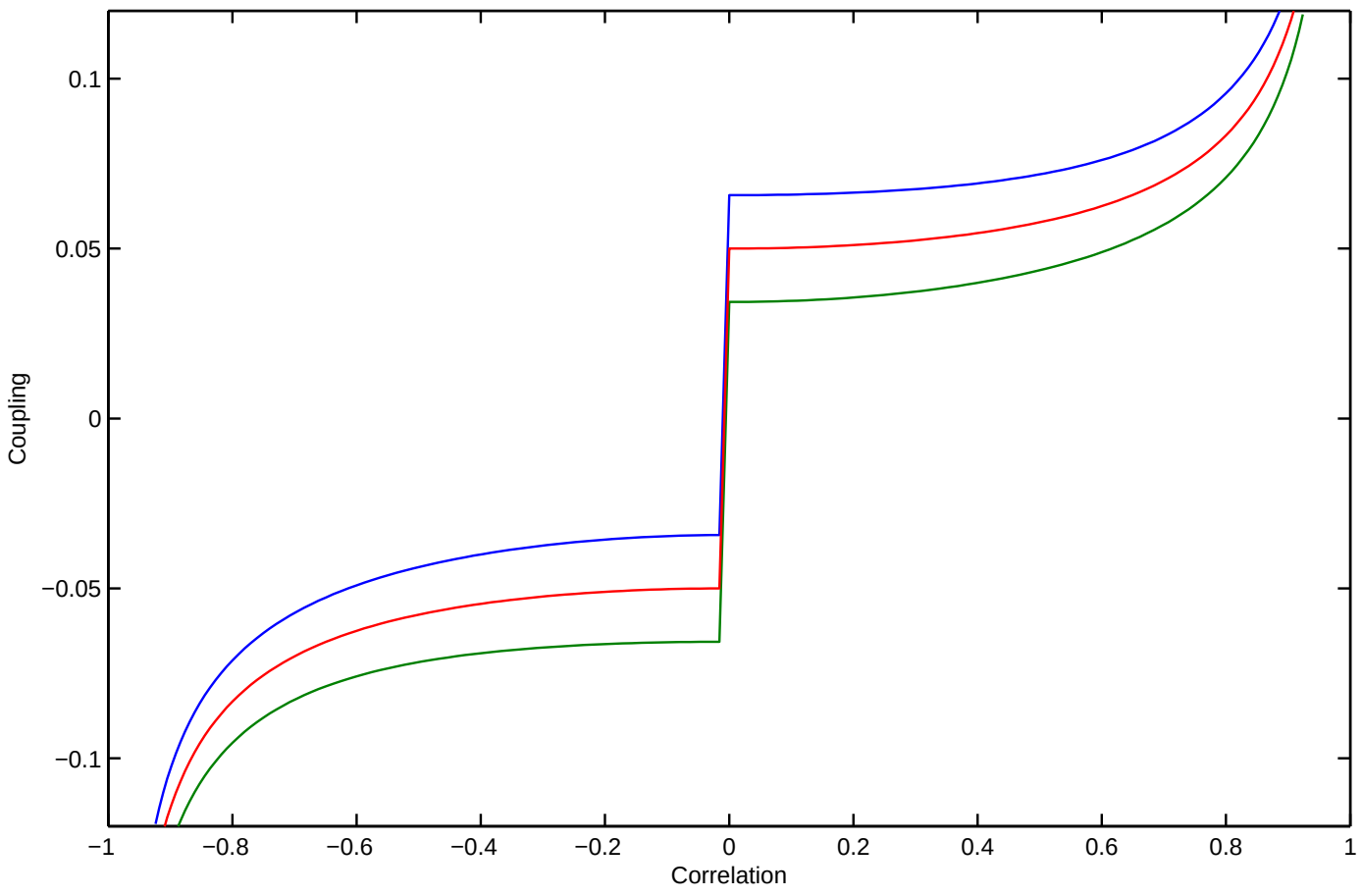

Figure3

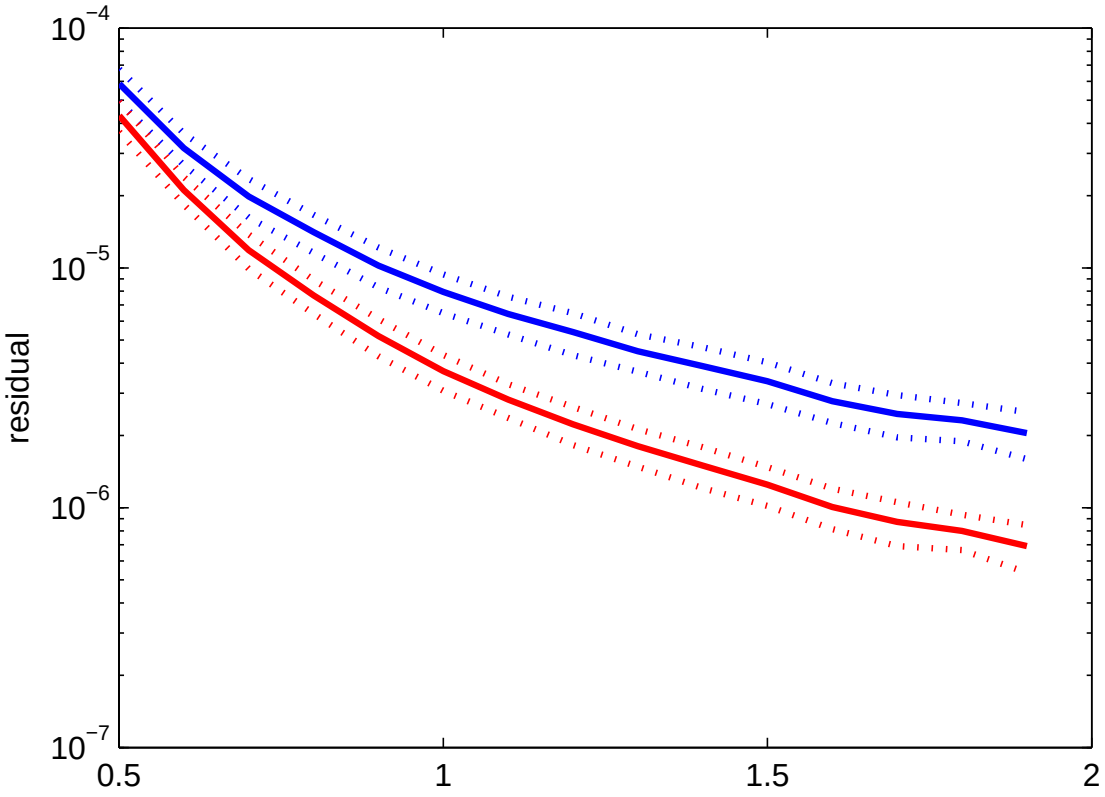
residual
$10^{-4}$
$10^{-5}$
$10^{-6}$
$10^{-7}$
0.5
1
1.5
2

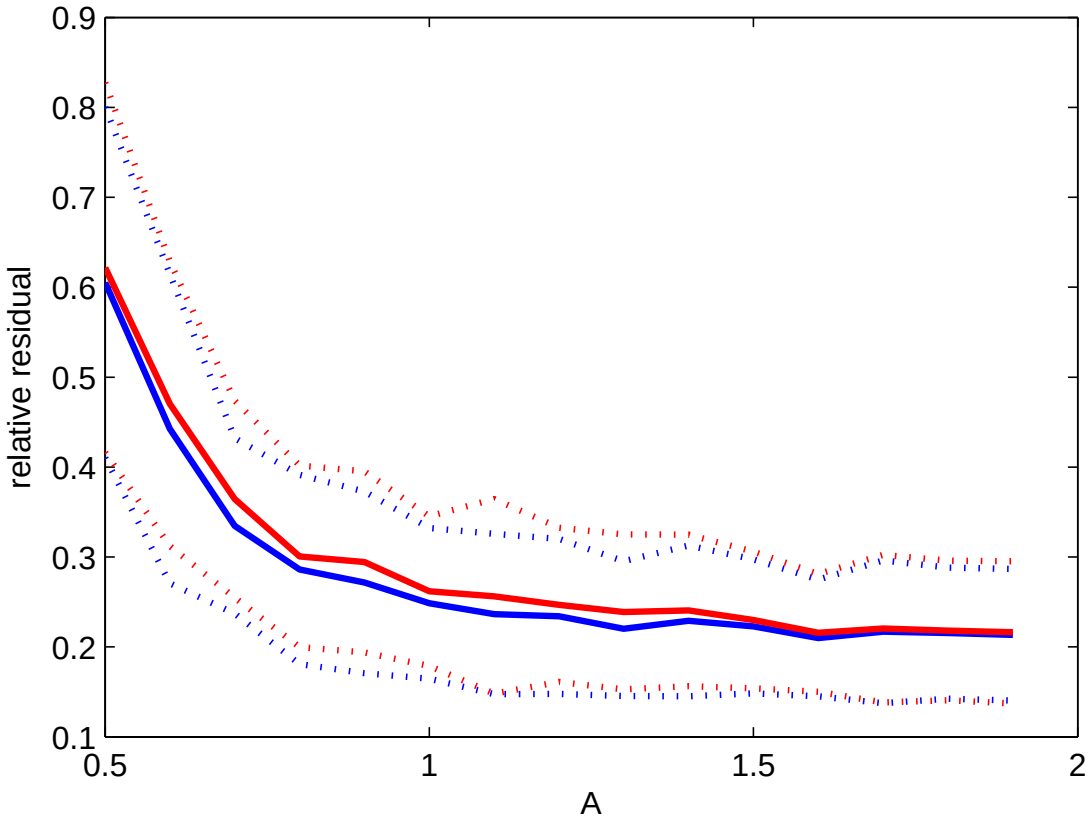
relative residual
0.9
0.8
0.7
0.6
0.5
0.4
0.3
0.2
0.1
0.5
1
1.5
2
A

Figure4

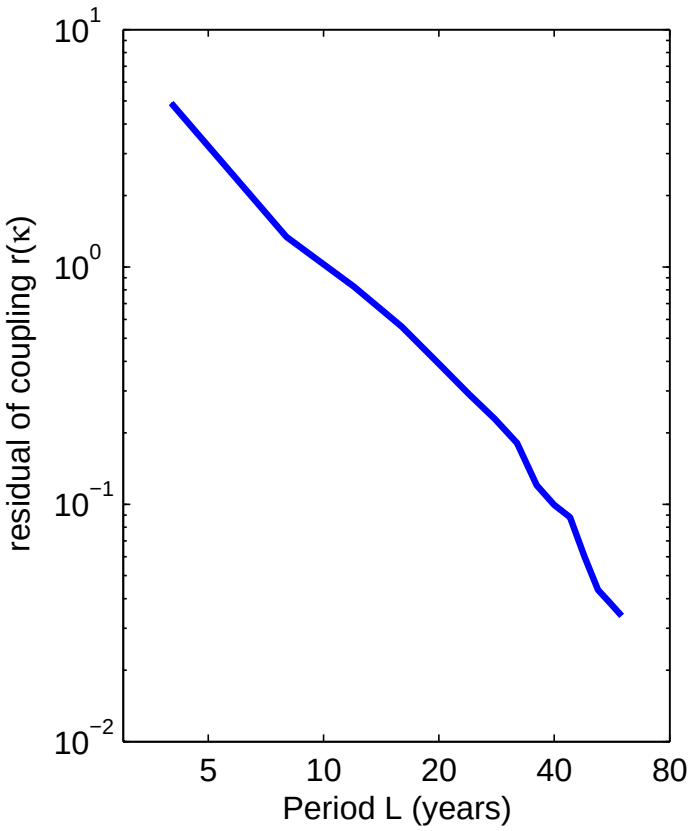
residual of coupling r(κ)
Period L (years)

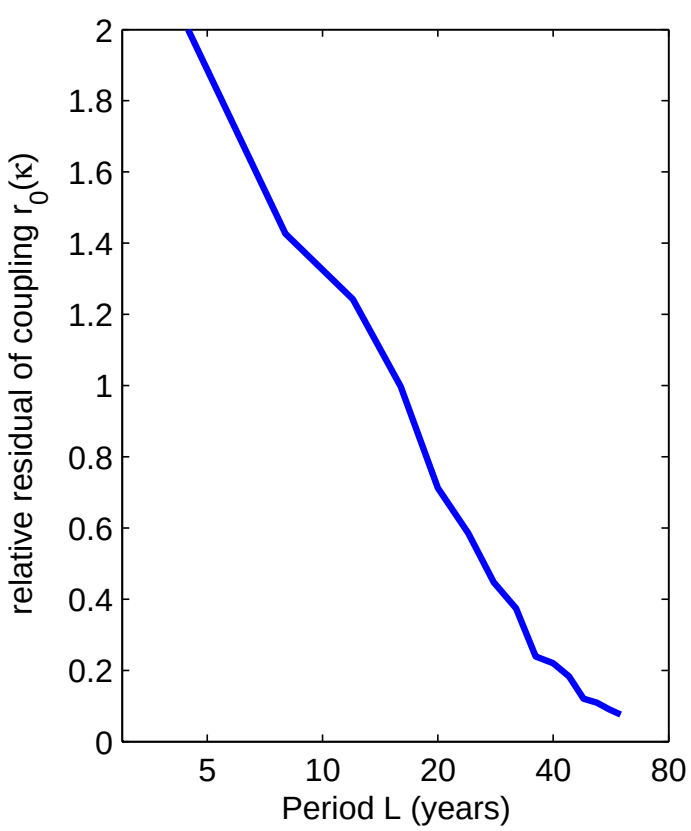
relative residual of coupling r0(κ)
Period L (years)

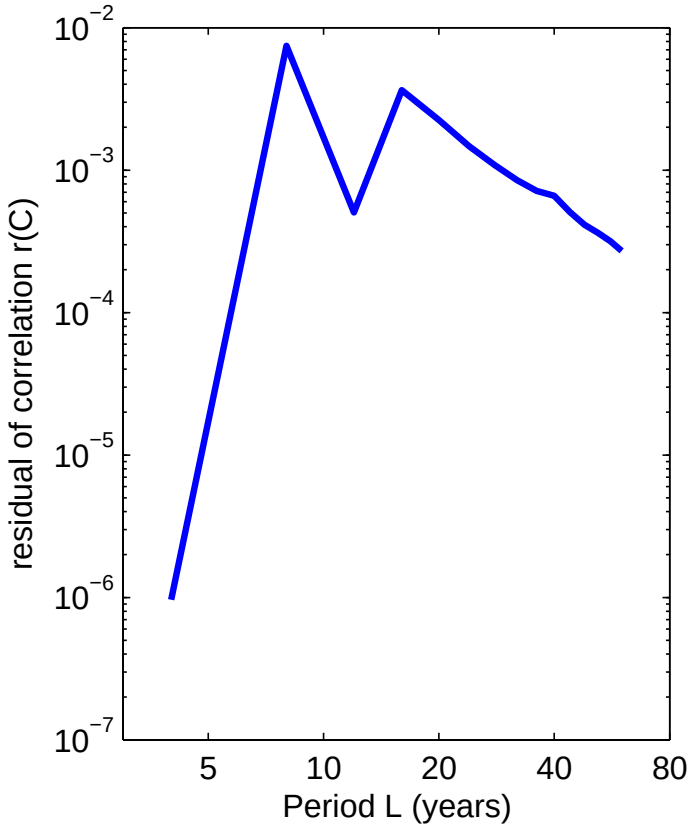
residual of correlation r(C)
Period L (years)

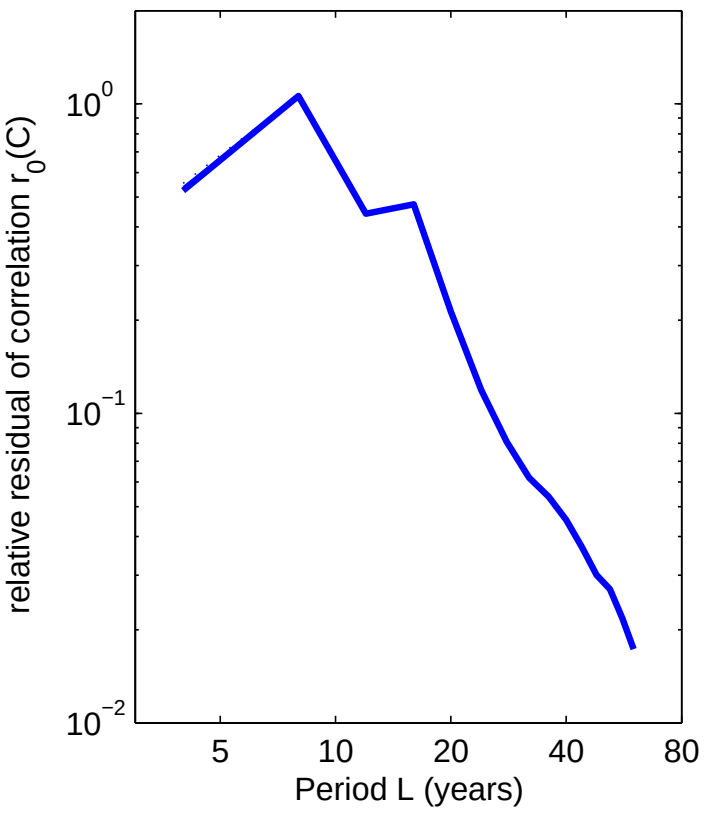
relative residual of correlation r0(C)
Period L (years)

Figure5

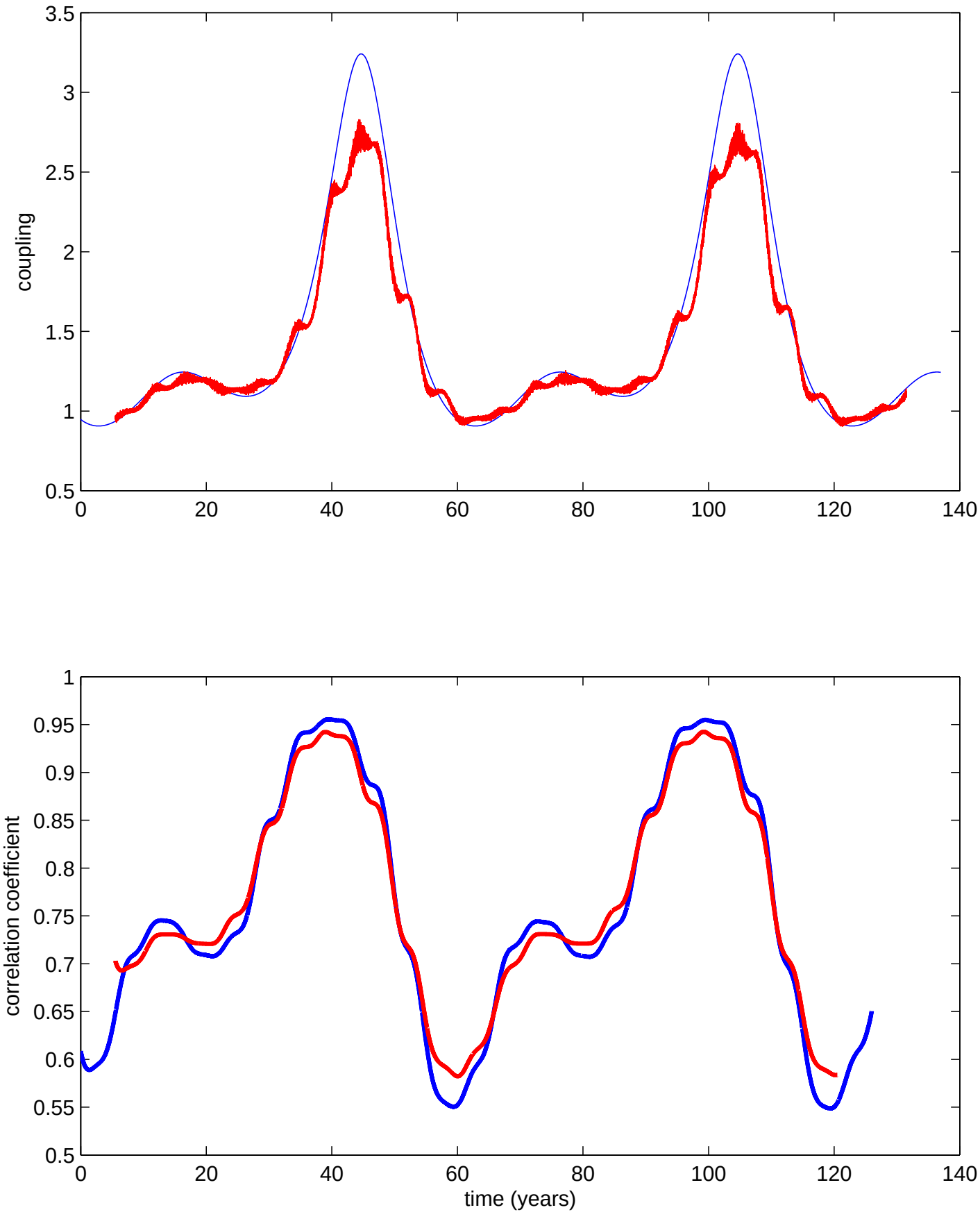
coupling
3.5
3
2.5
2
1.5
1
0.5
0
20
40
60
80
100
120
140
correlation coefficient
1
0.95
0.9
0.85
0.8
0.75
0.7
0.65
0.6
0.55
0.5
0
20
40
60
80
100
120
140
time (years)

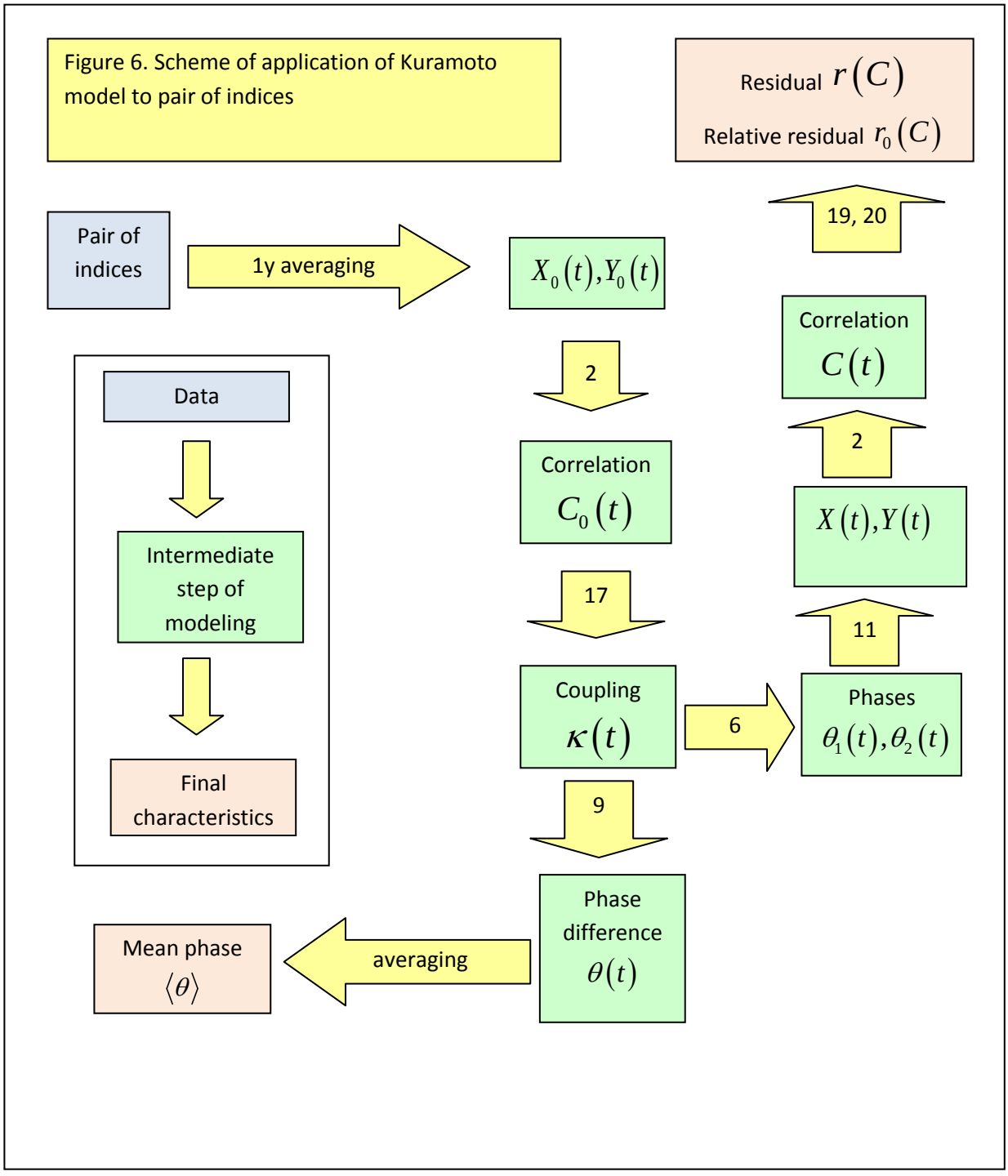
Figure 6. Scheme of application of Kuramoto model to pair of indices
Residual $r(C)$
Relative residual $r_0(C)$
19, 20
Pair of indices
1y averaging
$X_0(t), Y_0(t)$
Correlation $C(t)$
2
2
Data
Correlation $C_0(t)$
$X(t), Y(t)$
Intermediate step of modeling
17
11
Coupling $\kappa(t)$
6
Phases $\theta_1(t), \theta_2(t)$
Final characteristics
9
Phase difference $\theta(t)$
Mean phase $\langle\theta\rangle$
averaging

Figure7

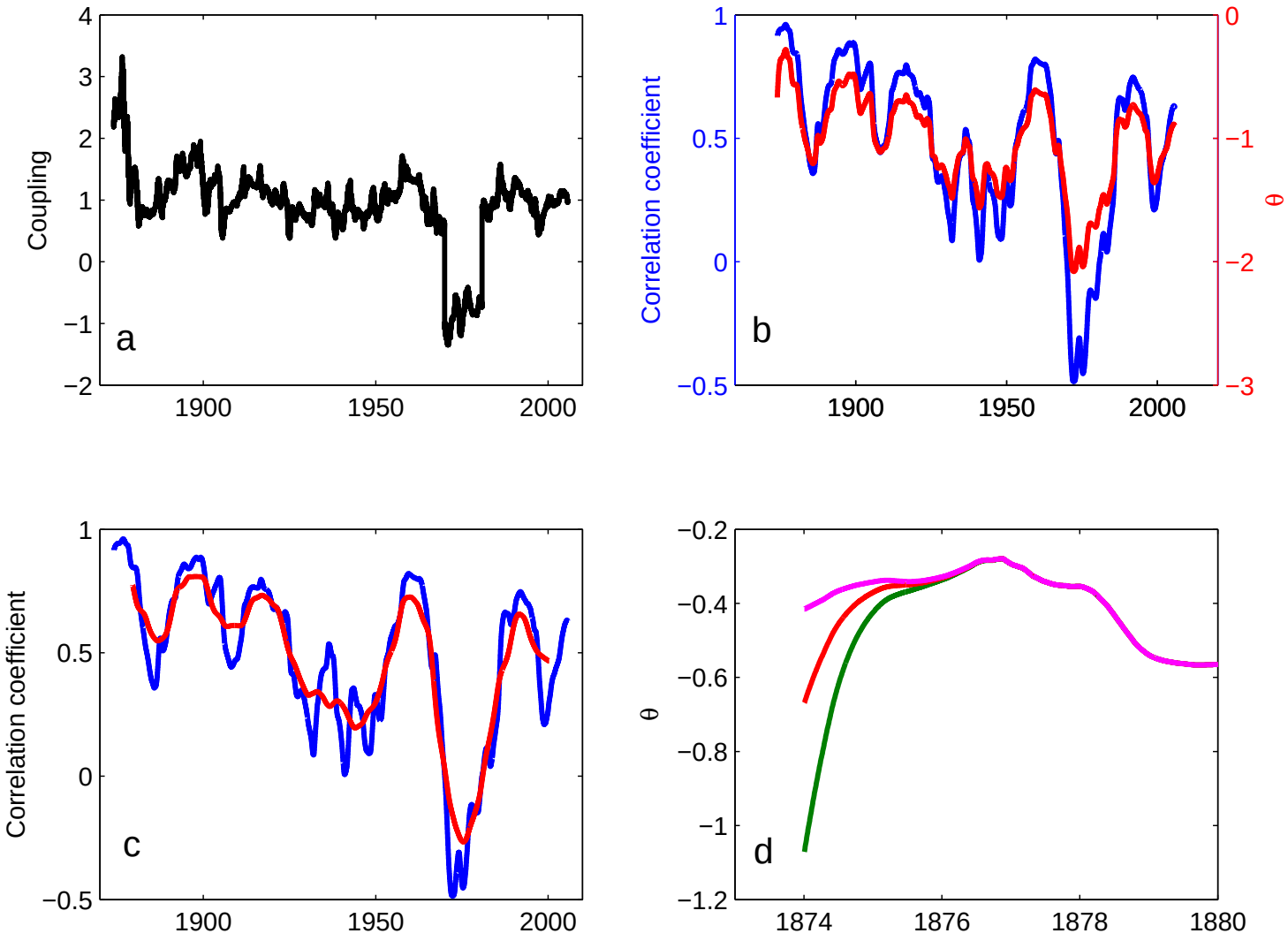
Coupling
a
1900
1950
2000
Correlation coefficient
θ
b
c
d
1874
1876
1878
1880

Figure8

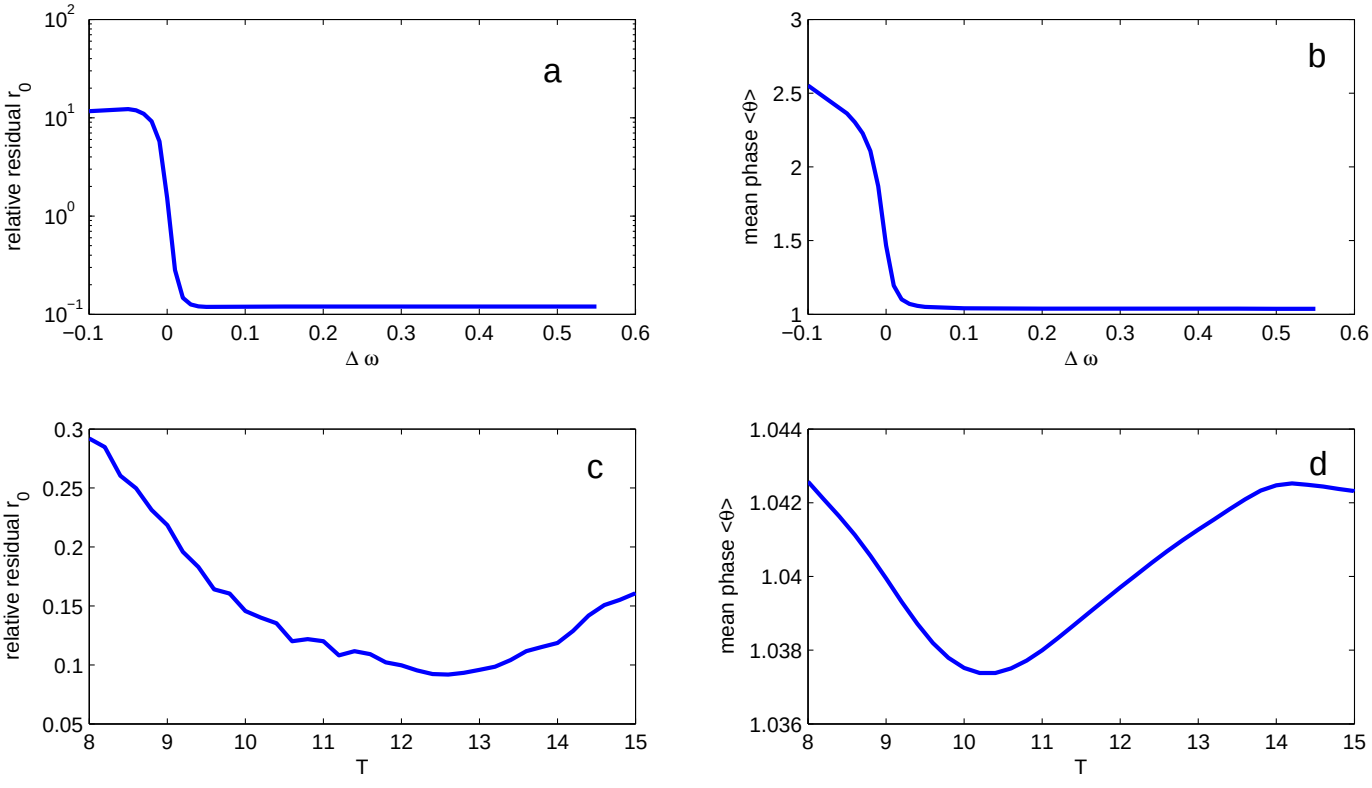

Figure9

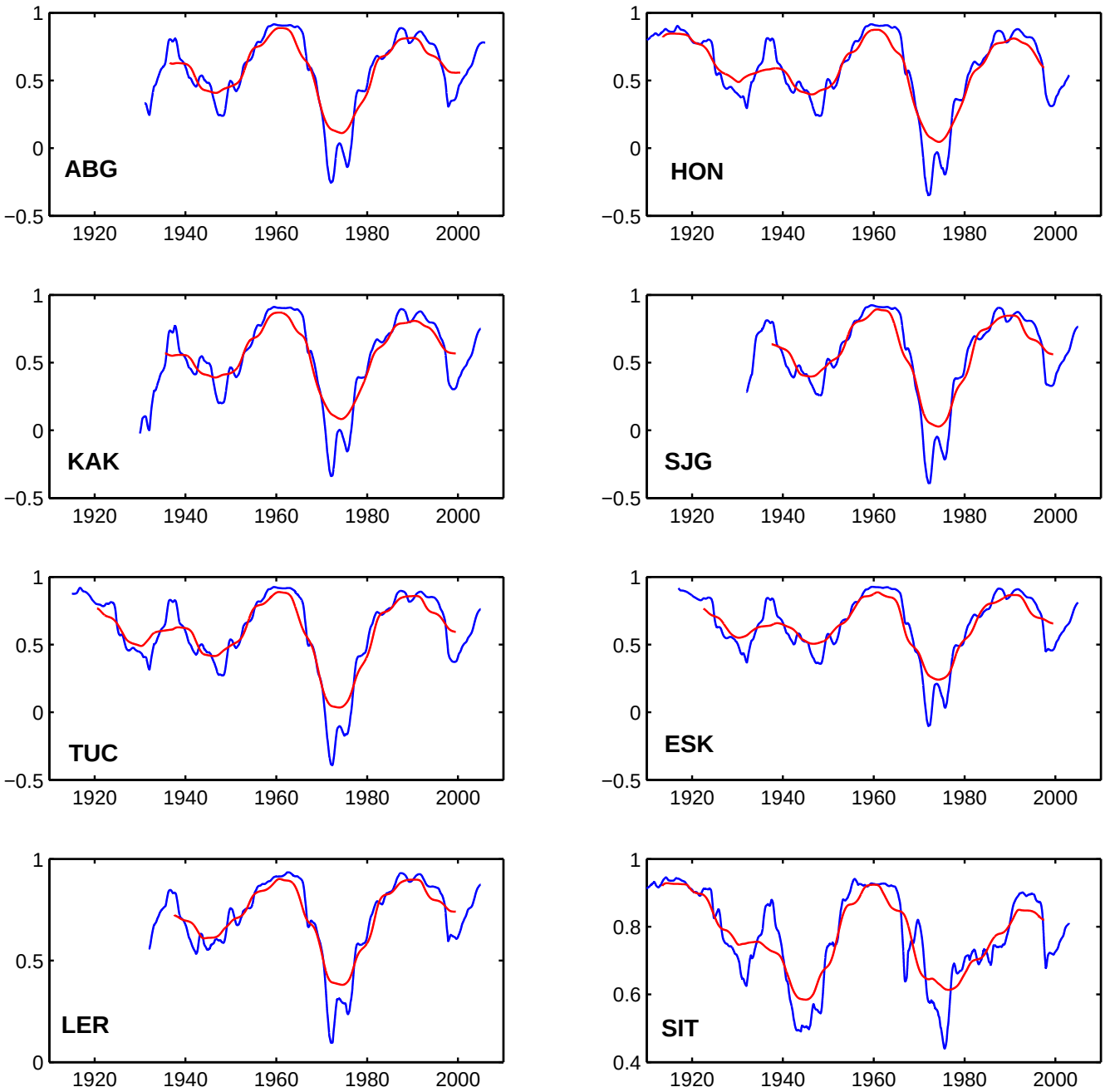
ABG
HON
KAK
SJG
TUC
ESK
LER
SIT
1
0.5
0
−0.5
0.8
0.6
0.4
1920
1940
1960
1980
2000

Figure10

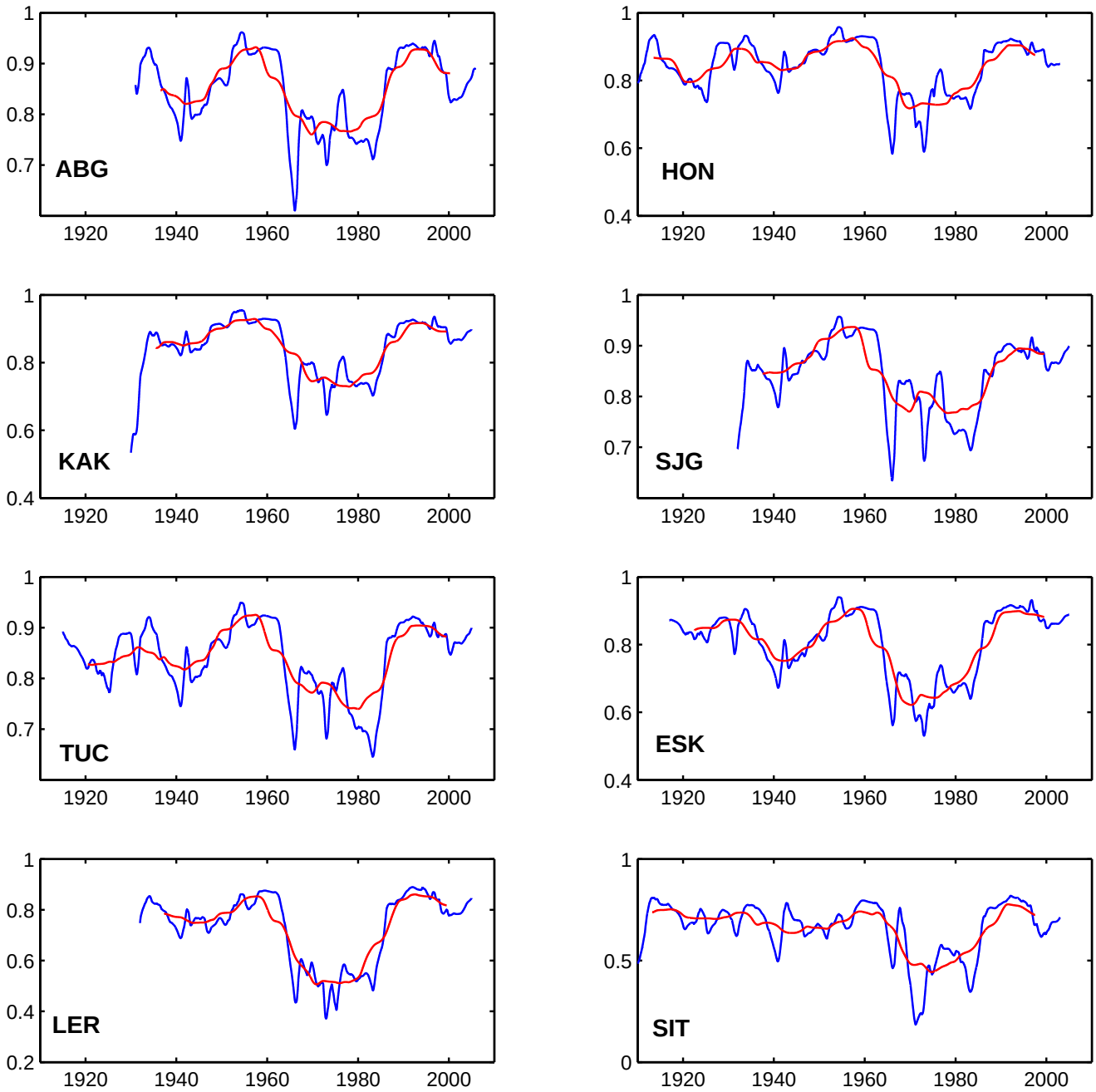

Figure11


ABG
HON
KAK
SJG
TUC
ESK
LER
SIT
3
2
1
0
−1
−2
1920
1940
1960
1980
2000

Figure12

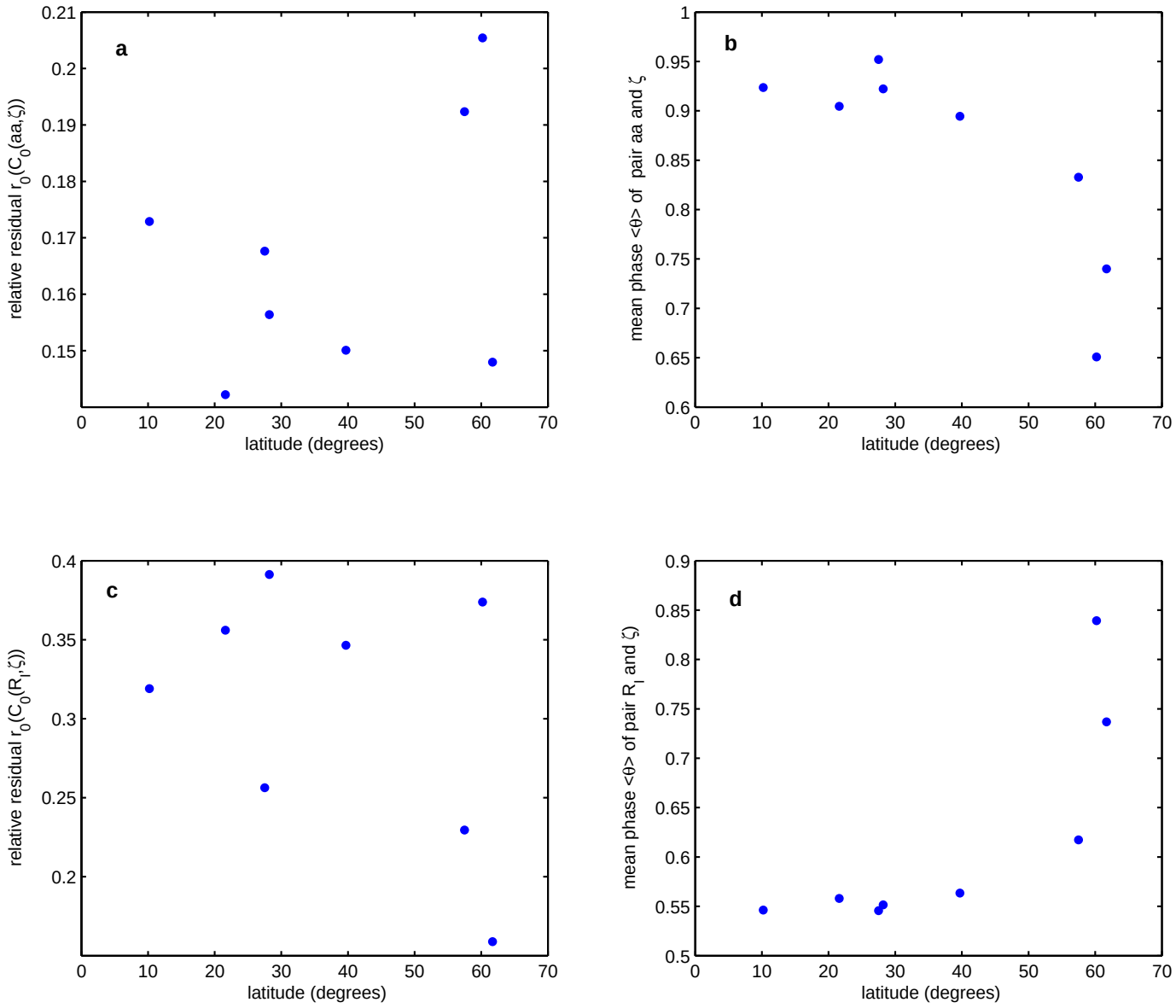
a
relative residual r0(C0(aa,ζ))
latitude (degrees)
b
mean phase <θ> of pair aa and ζ
latitude (degrees)
c
relative residual r0(C0(RI,ζ))
latitude (degrees)
d
mean phase <θ> of pair RI and ζ)
latitude (degrees)

Figure13

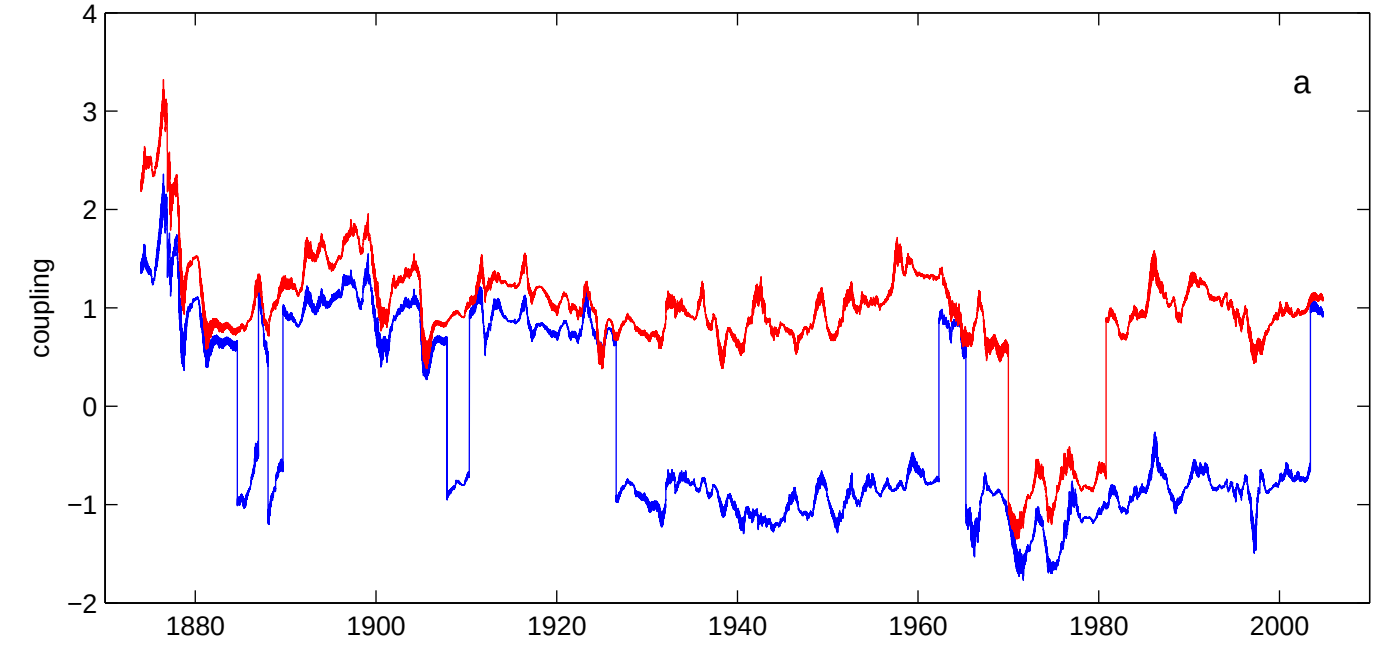
a
coupling
4
3
2
1
0
−1
−2
1880
1900
1920
1940
1960
1980
2000

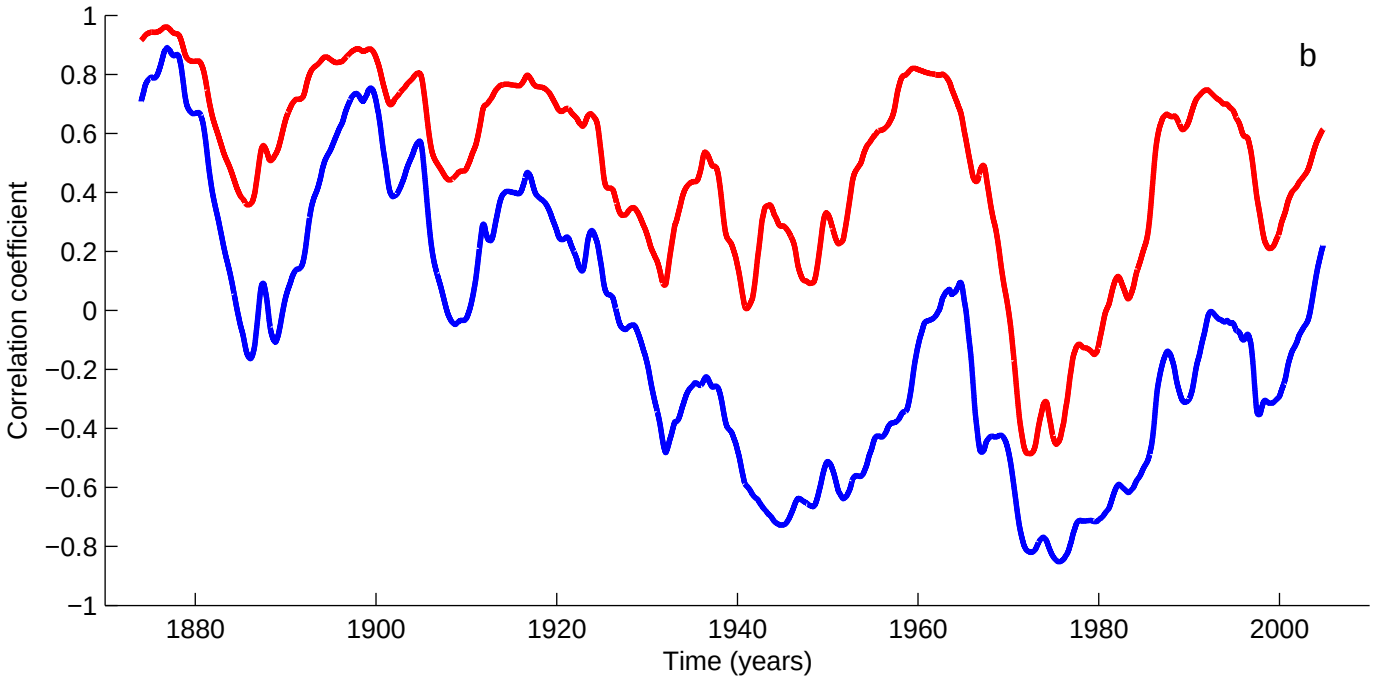
b
Correlation coefficient
1
0.8
0.6
0.4
0.2
0
−0.2
−0.4
−0.6
−0.8
−1
1880
1900
1920
1940
1960
1980
2000
Time (years)